

# Directed mixed membership stochastic blockmodel

**Huan Qing**

*School of Mathematics  
China University of Mining and Technology  
Xuzhou, 221116, P.R. China*

QINGHUAN@CUMT.EDU.CN

**Jingli Wang**

*School of Statistics and Data Science  
Nankai University  
Tianjin, 300071, P.R. China*

JLWANG@NANKAI.EDU.CN

**Editor:**

## Abstract

Mixed membership problem for undirected network has been well studied in network analysis recent years. However, the more general case of mixed membership for directed network in which nodes can belong to multiple communities remains a challenge. Here, we propose an interpretable and identifiable model: directed mixed membership stochastic blockmodel (DiMMSB) for directed mixed membership networks. DiMMSB allows that row nodes and column nodes of the adjacency matrix can be different and these nodes may have distinct community structure in a directed network. We also develop an efficient spectral algorithm called DiSP designed based on simplex structures inherent in the left and right singular vectors of the population adjacency matrix to estimate the mixed memberships for both row nodes and column nodes in a directed network. We show that DiSP is asymptotically consistent under mild conditions by providing error bounds for the inferred membership vectors of each row node and each column node using delicate spectral analysis. Numerical results on computer-generated directed mixed membership networks support our theoretical findings and show that our DiSP outperforms its competitor in both error rates and run-time. Applications of DiSP to real-world directed networks demonstrate the advantages of DiSP in studying the asymmetric structure of directed networks.

**Keywords:** Community detection, Ideal Simplex, overlapping directed network, sparsity, spectral clustering, SVD.

## 1. Introduction

Networks with meaningful structures are ubiquitous in our daily life in the big data era. For example, the social networks generated by social platforms (such as, Facebook, Twitter, Wechat, Instagram, WhatsUp, Line, etc) provide relationships or friendships among users; the protein-protein interaction networks record the relationships among proteins; the citation networks reflect authors' research preferences Dunne et al. (2002); Newman (2004); Notebaart et al. (2006); Pizzuti (2008); Gao et al. (2010); Lin et al. (2012); Su et al. (2010); Scott and Carrington (2014); Bedi and Sharma (2016); Wang et al. (2020). To analyze networks mathematically, researchers present them in a form of graph in which subjects/individuals are presented by nodes, and the relationships are measured by the edges,

directions of edges and weights. Community detection is one of the major tools to extract structural information from these networks.

For simplification, most researchers study the undirected networks for community detection such as Lancichinetti and Fortunato (2009); Goldenberg et al. (2010); Karrer and Newman (2011); Qin and Rohe (2013); Lei and Rinaldo (2015); Jin (2015); Chen et al. (2018). The Stochastic Blockmodel (SBM) Holland et al. (1983) is a classical and widely used model to generate undirected networks. SBM assumes that one node only belongs to one community and the probability of a link between two nodes depends only on the communities memberships of the two nodes. SBM also assumes the nodes within each community have the same expected degrees. Abbe (2017) proposed a review on recent developments about SBM. While, in real cases some nodes may share among multiple communities with different degrees, which is known as mixed membership (also known as overlapping) networks. Airoldi et al. (2008) extended SBM to mixed membership networks and designed the Mixed Membership Stochastic Blockmodel (MMSB). Substantial algorithms have been developed based on MMSB, such as Gopalan and Blei (2013); Jin et al. (2017); Mao et al. (2017, 2020); Zhang et al. (2020).

Directed networks such as citation networks, protein-protein interaction networks and the hyperlink network of websites are also common in our life. Such directed networks are more complex since they often involve two types of information, sending nodes and receiving nodes. For instance, in a citation network, one paper may cite many other papers, then this paper can be labeled as ‘sending node’ and these cited papers can be labeled as ‘receiving nodes’. Several interesting works have been developed for directed networks. Rohe et al. (2016) proposed a model called Stochastic co-Blockmodel (ScBM) to model networks with directed (asymmetric) relationships where nodes have no mixed memberships (i.e., one node only belongs to one community). Wang et al. (2020) studied the theoretical guarantee for the algorithm D-SCORE Ji and Jin (2016) which is designed based on the degree-corrected version of ScBM. Lim et al. (2018) proposed a flexible noise tolerant graph clustering formulation based on non-negative matrix factorization (NMF), which solves graph clustering such as community detection for either undirected or directed graphs. In the bipartite setting some authors constructed new models by extending SBM, such as Zhou and Amini (2018); Razaee et al. (2019). The above models and algorithms for directed network community detection focus on non-mixed membership directed networks. Similar as in undirected networks, in reality, there exist a lot of directed networks such that their sending nodes and/or receiving nodes may belong to multiple clusters.

For the directed network with mixed memberships, Airoldi et al. (2013) proposed a multi-way stochastic blockmodel with Dirichlet distribution which is an extension of the MMSB model Airoldi et al. (2008), and applied the nonparametric methods, collapsed Gibbs sampling and variational Expectation-Maximization to make inference. In this paper, we focus on the directed network with mixed memberships and aim at developing a provably consistent spectral algorithm to estimate network memberships.

Our contributions in this paper are as follows:

- (i) We propose a generative model for directed networks with mixed memberships, the Directed Mixed Membership Stochastic Blockmodel (DiMMSB for short). DiMMSB allows that nodes in a directed network can belong to multiple communities. The proposed model also allows that sending nodes (row nodes) and receiving nodes (column

nodes) can be different, that is, the adjacency matrix could be a non-square matrix. The identifiability of DiMMSB is verified under common constraints for mixed membership models.

- (ii) We construct a fast spectral algorithm, DiSP, to fit DiMMSB. DiSP is designed based on the investigation that there exist a Row Ideal Simplex structure and a Column Ideal Simplex structure in the right singular vectors and the left singular vectors of the population adjacency matrix. To scale the sparsity of a directed mixed membership network, we introduce the sparsity parameter. By taking the advantage of the recent row-wise singular vector deviation Chen et al. (2020) and the equivalence algorithm of DiSP, we obtain the upper bounds of error rates for each row node and each column node, and show that our method produces asymptotically consistent parameter estimations under mild conditions on the network sparsity by delicate spectral analysis. To our knowledge, this is the first work to establish consistent estimation for an estimation algorithm for directed mixed membership (overlapping) network models. Meanwhile, numerical results on substantial simulated directed mixed membership networks show that DiSP is useful and fast in estimating mixed memberships, and results on real-world data demonstrate the advantages on DiSP in studying the asymmetric structure and finding highly mixed nodes in a directed network.

**Notations.** We take the following general notations in this paper. For a vector  $x$ ,  $\|x\|_q$  denotes its  $l_q$ -norm.  $M'$  is the transpose of the matrix  $M$ , and  $\|M\|$  denotes the spectral norm, and  $\|M\|_F$  denotes the Frobenius norm.  $\|X\|_{2 \rightarrow \infty}$  denotes the maximum  $l_2$ -norm of all the rows of the matrix  $X$ . Let  $\sigma_i(M)$  and  $\lambda_i(M)$  be the  $i$ -th largest singular value and its corresponding eigenvalue of matrix  $M$  ordered by the magnitude.  $M(i, :)$  and  $M(:, j)$  denote the  $i$ -th row and the  $j$ -th column of matrix  $M$ , respectively.  $M(S_r, :)$  and  $M(:, S_c)$  denote the rows and columns in the index sets  $S_r$  and  $S_c$  of matrix  $M$ , respectively. For any matrix  $M$ , we simply use  $Y = \max(0, M)$  to represent  $Y_{ij} = \max(0, M_{ij})$  for any  $i, j$ .

## 2. The directed mixed membership stochastic blockmodel

In this section we introduce the directed mixed membership stochastic blockmodel. First we define a bi-adjacency matrix  $A \in \{0, 1\}^{n_r \times n_c}$  such that for each entry,  $A(i, j) = 1$  if there is a directional edge from row node  $i$  to column node  $j$ , and  $A(i, j) = 0$  otherwise, where  $n_r$  and  $n_c$  indicate the number of rows and the number of columns, respectively (the followings are similar). So, the  $i$ -th row of  $A$  records how row node  $i$  sends edges, and the  $j$ -th column of  $A$  records how column node  $j$  receives edges. Let  $S_r = \{i : i \text{ is a row node}, 1 \leq i \leq n_r\}$ , and  $S_c = \{j : j \text{ is a column node}, 1 \leq j \leq n_c\}$ . In this paper, we assume that the row (sending) nodes can be different from the column (receiving) nodes, and the number of row nodes and the number of columns are not necessarily equal. We assume the row nodes of  $A$  belong to  $K$  perceivable communities (call row communities and we also call them sending clusters occasionally in this paper)

$$\mathcal{C}_r^{(1)}, \mathcal{C}_r^{(2)}, \dots, \mathcal{C}_r^{(K)}, \tag{1}$$

and the column nodes of  $A$  belong to  $K$  perceivable communities (call column communities and we also call them receiving clusters occasionally in this paper)

$$\mathcal{C}_c^{(1)}, \mathcal{C}_c^{(2)}, \dots, \mathcal{C}_c^{(K)}. \quad (2)$$

Let  $\Pi_r \in \mathbb{R}^{n_r \times K}$  and  $\Pi_c \in \mathbb{R}^{n_c \times K}$  be row nodes membership matrix and column nodes membership matrix respectively, such that  $\Pi_r(i, :)$  is a  $1 \times K$  Probability Mass Function (PMF) for row node  $i$ ,  $\Pi_c(j, :)$  is a  $1 \times K$  PMF for column node  $j$ , and

$$\Pi_r(i, k) \text{ is the weight of row node } i \text{ on } \mathcal{C}_r^{(k)}, 1 \leq k \leq K, \quad (3)$$

$$\Pi_c(j, k) \text{ is the weight of column node } j \text{ on } \mathcal{C}_c^{(k)}, 1 \leq k \leq K. \quad (4)$$

We call row node  $i$  ‘pure’ if  $\Pi_r(i, :)$  degenerates (i.e., one entry is 1, all others  $K - 1$  entries are 0) and ‘mixed’ otherwise. Same definitions hold for column nodes.

Define a *probability matrix*  $P \in \mathbb{R}^{K \times K}$  which is a nonnegative matrix and for any  $1 \leq k, l \leq K$ ,

$$P(k, l) \in [0, 1]. \quad (5)$$

Note that since we consider directed mixed membership network in this paper,  $P$  may be asymmetric. For all pairs of  $(i, j)$  with  $1 \leq i \leq n_r, 1 \leq j \leq n_c$ , DiMMSB assumes that  $A(i, j)$  are independent Bernoulli random variables satisfying

$$\mathbb{P}(A(i, j) = 1) = \sum_{k=1}^K \sum_{l=1}^K \Pi_r(i, k) \Pi_c(j, l) P(k, l). \quad (6)$$

**Definition 1** Call model (1)-(6) as the *Directed Mixed Membership Stochastic Blockmodel (DiMMSB)* and denote it by  $DiMMSB(n_r, n_c, K, P, \Pi_r, \Pi_c)$ .

DiMMSB can be deemed as an extension of some previous models.

- When all row nodes and column nodes are pure, our DiMMSB reduces to ScBM with  $K$  row clusters and  $K$  column clusters Rohe et al. (2016).
- When  $\Pi_r(i, :)$  and  $\Pi_c(j, :)$  follow Dirichlet distribution for  $1 \leq i \leq n_r$  and  $1 \leq j \leq n_c$ , DiMMSB reduces to the two-way stochastic blockmodels with Bernoulli distribution Airoldi et al. (2013).
- When  $\Pi_r = \Pi_c$  and  $P = P'$ ,  $\Pi_r(i, :)$  follow Dirichlet distribution for  $1 \leq i \leq n_r$ , and all row nodes and column nodes are the same, DiMMSB reduces to MMSB Airoldi et al. (2008).
- When  $\Pi_r = \Pi_c$  and  $P = P'$ , all row nodes and column nodes are the same, and all nodes are pure, DiMMSB reduces to SBM Holland et al. (1983).

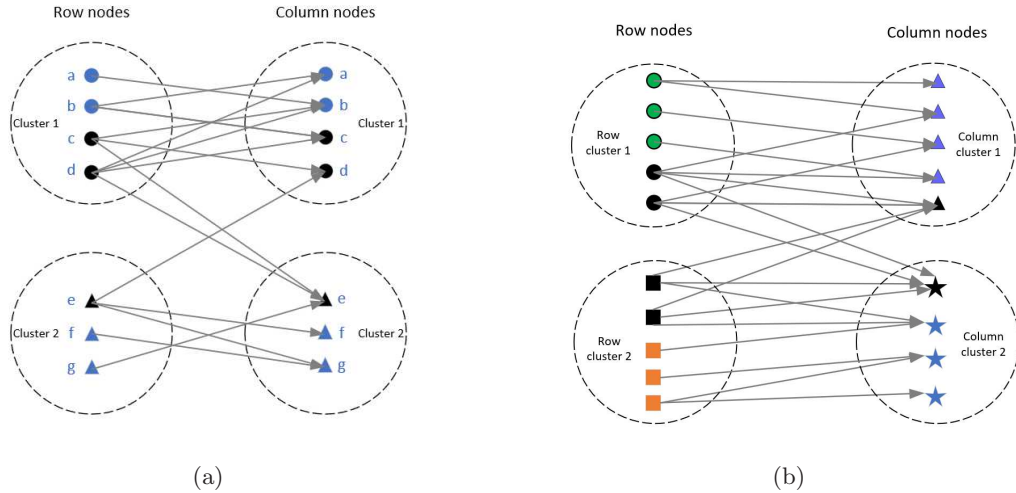


Figure 1: Two schematic diagrams for DiMMSB.

DiMMSB can model various networks, and the generality of DiMMSB can be laconically explained by the two schematic diagrams in Figure 1. In the figure, an arrow demonstrates a directed edge from one node to another, nodes in the same cluster are enclosed by dashed circle, and nodes in black have mixed memberships. In panel (a) of Figure 1, row nodes and column nodes are the same, 7 nodes in this network (i.e.,  $A \in \mathbb{R}^{7 \times 7}$ ), nodes  $a, b, c, d$  belong to row cluster 1 and they also belong to column cluster 1, and nodes  $e, f, g$  belong to row cluster 2 and column cluster 2. Since nodes  $c$  and  $d$  point to nodes  $e$ , node  $e$  points to node  $d$ , these three nodes  $c, d, e$  have mixed memberships. In panel (b), row nodes are different from column nodes. There are 10 row nodes where nodes referred by solid circle belong to row cluster 1, and nodes referred by solid square belong to row cluster 2. There are 9 column nodes where nodes referred by solid triangle belong to column cluster 1, and nodes referred by solid star belong to column cluster 2. The directed adjacency matrix  $A$  in panel (b) is a  $10 \times 9$  matrix, whose row nodes are different from column nodes. Meanwhile, for row nodes, since the black circles and the black squares point to the black triangle node and the black star node, they are mixed row nodes. Since the black triangle node and the black star node are pointed by mixed nodes, they are treated as mixed column nodes. Meanwhile, works in Rohe et al. (2016); Zhou and A.Amini (2019); Razaee et al. (2019); Zhou and Amini (2020); Ndaoud et al. (2021) also consider the general case when row nodes may differ column nodes for their theoretical analysis.

## 2.1 Identifiability

The parameters in the DiMMSB model obviously need to be constrained to guarantee identifiability of the model. All models with communities, are considered identifiable if they are identifiable up to a permutation of community labels Jin et al. (2017); Zhang et al. (2020); Mao et al. (2020). The following conditions are sufficient for the identifiability of DiMMSB:

- (I1)  $\text{rank}(P) = K$ .
- (I2) There is at least one pure node for each of the  $K$  row and  $K$  column communities.

The full rank condition (I1) for connectivity matrix  $P$  and pure nodes condition (I2) are popular conditions for models modeling network with mixed memberships, see Jin et al. (2017); Zhang et al. (2020); Mao et al. (2018, 2020). Now we decompose  $A$  into a sum of a ‘signal’ part and a ‘noise’ part:

$$A = \Omega + W,$$

where the  $n_r \times n_c$  matrix  $\Omega$  is the expectation of the adjacency matrix  $A$ , and  $W$  is a generalized Wigner matrix. Then, under DiMMSB, we have

$$\Omega = \Pi_r P \Pi_c'. \tag{7}$$

We refer  $\Omega$  as the population adjacency matrix. By basic algebra, we know  $\Omega$  is of rank  $K$ . Thus  $\Omega$  is a low-rank matrix ( $K < \min\{n_r, n_c\}$ ) which is the key for why spectral clustering method works for DiMMSB.

Next proposition guarantees that when conditions (I1) and (I2) hold, DiMMSB is identifiable.

**Proposition 1** *If conditions (I1) and (I2) hold, DiMMSB is identifiable, i.e., if a given matrix  $\Omega$  corresponds to a set of parameters  $(n_r, n_c, K, P, \Pi_r, \Pi_c)$  through (7), these parameters are unique up to a permutation of community labels.*

Unless specified, we treat conditions (I1) and (I2) as default from now on.

## 2.2 Sparsity scaling

Real-world large scale networks are usually sparse, in the sense that the number of edges from a node (the node degree) are very small compared to the total number of nodes. Generally speaking, community recovery is hard when the data set is sparse. As a result, an important criterion of evaluating a community recovery method is its performance under different levels of sparsity. In this paper, we capture the sparsity of a directed mixed membership network by the sparsity parameter  $\rho$  such that

$$P = \rho \tilde{P} \text{ where } \max_{1 \leq k, l \leq K} \tilde{P}(k, l) = 1.$$

Under  $DiMMSB(n_r, n_c, K, P, \Pi_r, \Pi_c)$ , a smaller  $\rho$  leads to a smaller probability to generate an edge from row node  $i$  to column node  $j$ , i.e., the sparsity parameter  $\rho$  captures the sparsity behaviors for generating a directed mixed membership network. When building theoretical guarantee on estimation consistency of spectral clustering methods in community detection, controlling the sparsity of a network is common, see Lei and Rinaldo (2015); Jin (2015); Rohe et al. (2016); Mao et al. (2020); Wang et al. (2020). Especially, when DiMMSB degenerates to SBM, Assumption 1 matches the sparsity requirement in Theorem 3.1 Lei and Rinaldo (2015), and this guarantees the optimality of our sparsity condition. Meanwhile, as mentioned in Jin et al. (2017); Mao et al. (2020),  $\sigma_K(\tilde{P})$  is a measure of the separation between communities and a larger  $\sigma_K(\tilde{P})$  gives more well-separated communities. This paper also aims at studying the effect of  $\rho$  and  $\sigma_K(\tilde{P})$  on the performance of spectral clustering by allowing them to be contained in the error bound. Therefore, our theoretical results allow model parameters  $K, \rho, \sigma_K(\tilde{P})$  to vary with  $n_r$  and  $n_c$ .



### 3. A spectral algorithm for fitting DiMMSB

The primary goal of the proposed algorithm is to estimate the row membership matrix  $\Pi_r$  and column membership matrix  $\Pi_c$  from the observed adjacency matrix  $A$  with given  $K$ . Considering the computational scalability, we focus on the idea of spectral clustering by spectral decomposition to design an efficient algorithm under DiMMSB in this paper.

We now discuss our intuition for the design of our algorithm. Under conditions (I1) and (I2), by basic algebra, we have  $\text{rank}(\Omega) = K$ , which is much smaller than  $\min\{n_r, n_c\}$ . Let  $\Omega = U\Lambda V'$  be the compact singular value decomposition (SVD) of  $\Omega$ , where  $U \in \mathbb{R}^{n_r \times K}$ ,  $\Lambda \in \mathbb{R}^{K \times K}$ ,  $V \in \mathbb{R}^{n_c \times K}$ ,  $U'U = I_K$ ,  $V'V = I_K$ , and  $I_K$  is a  $K \times K$  identity matrix. For  $1 \leq k \leq K$ , let  $\mathcal{I}_r^{(k)} = \{i \in \{1, 2, \dots, n_r\} : \Pi_r(i, k) = 1\}$  and  $\mathcal{I}_c^{(k)} = \{j \in \{1, 2, \dots, n_c\} : \Pi_c(j, k) = 1\}$ . By condition (I2),  $\mathcal{I}_r^{(k)}$  and  $\mathcal{I}_c^{(k)}$  are non empty for all  $1 \leq k \leq K$ . For  $1 \leq k \leq K$ , select one row node from  $\mathcal{I}_r^{(k)}$  to construct the index set  $\mathcal{I}_r$ , i.e.,  $\mathcal{I}_r$  is the indices of row nodes corresponding to  $K$  pure row nodes, one from each community. And  $\mathcal{I}_c$  is defined similarly. W.L.O.G., let  $\Pi_r(\mathcal{I}_r, :) = I_K$  and  $\Pi_c(\mathcal{I}_c, :) = I_K$  (Lemma 2.1 in Mao et al. (2020) also has similar setting to design their spectral algorithms under MMSB.). The existences of the Row Ideal Simplex (RIS for short) structure inherent in  $U$  and the Column Ideal Simplex (CIS for short) structure inherent in  $V$  are guaranteed by the following lemma.

**Lemma 1** (*Row Ideal Simplex and Column Ideal Simplex*). *Under DiMMSB( $n_r, n_c, K, P, \Pi_r, \Pi_c$ ), there exist an unique  $K \times K$  matrix  $B_r$  and an unique  $K \times K$  matrix  $B_c$  such that*

- $U = \Pi_r B_r$  where  $B_r = U(\mathcal{I}_r, :)$ . Meanwhile,  $U(i, :) = U(\bar{i}, :)$ , if  $\Pi_r(i, :) = \Pi_r(\bar{i}, :)$  for  $1 \leq i, \bar{i} \leq n_r$ .
- $V = \Pi_c B_c$  where  $B_c = V(\mathcal{I}_c, :)$ . Meanwhile,  $V(j, :) = V(\bar{j}, :)$ , if  $\Pi_c(j, :) = \Pi_c(\bar{j}, :)$  for  $1 \leq j, \bar{j} \leq n_c$ .

Lemma 1 says that the rows of  $U$  form a  $K$ -simplex in  $\mathbb{R}^K$  which we call the Row Ideal Simplex (RIS), with the  $K$  rows of  $B_r$  being the vertices. Similarly, rows of  $V$  form a  $K$ -simplex in  $\mathbb{R}^K$  which we call the Column Ideal Simplex (CIS), with the  $K$  rows of  $B_c$  being the vertices. Meanwhile,  $U(i, :)$  is a convex linear combination of  $B_r(1, :), B_r(2, :), \dots, B_r(K, :)$  for  $1 \leq i \leq n_r$ . If row node  $i$  is pure,  $U(i, :)$  falls exactly on one of the vertices of the RIS. If row node  $i$  is mixed,  $U(i, :)$  is in the interior or face of the RIS, but not on any of the vertices. Similar conclusions hold for column nodes.

Since  $B_r$  and  $B_c$  are full rank matrices, if  $U, V, B_r$  and  $B_c$  are known in advance ideally, we can exactly obtain  $\Pi_r$  and  $\Pi_c$  by setting  $\Pi_r = UB_r'(B_r B_r')^{-1}$  and  $\Pi_c = VB_c'(B_c B_c')^{-1}$ .

While in practice, the estimation of  $UB_r'(B_r B_r')^{-1}$  and  $VB_c'(B_c B_c')^{-1}$  may not have unit row norm, thus we need to make the following transformation: Set  $Y_r = UB_r'(B_r B_r')^{-1}$ , and  $Y_c = VB_c'(B_c B_c')^{-1}$ . Then the membership matrices can be estimated by

$$\Pi_r(i, :) = \frac{Y_r(i, :)}{\|Y_r(i, :)\|_1}, \Pi_c(j, :) = \frac{Y_c(j, :)}{\|Y_c(j, :)\|_1}, 1 \leq i \leq n_r, 1 \leq j \leq n_c.$$

By the RIS structure  $U = \Pi_r B_r \equiv \Pi_r U(\mathcal{I}_r, :)$ , as long as we can obtain the row corner matrix  $U(\mathcal{I}_r, :)$  (i.e.,  $B_r$ ), we can recover  $\Pi_r$  exactly. As mentioned in Jin et al. (2017)

and Mao et al. (2020), for such ideal simplex, the successive projection (SP) algorithm Gillis and Vavasis (2015) (for details of SP, see Algorithm 4) can be applied to  $U$  with  $K$  row communities to find  $B_r$ . The above analysis gives how to recover  $\Pi_r$  with given  $\Omega$  and  $K$  under DiMMSB ideally. Similarly,  $\Pi_c$  can be exactly recovered by applying SP on all rows of  $V$  with  $K$  column communities.

Based on the above analysis, we are now ready to give the following three-stage algorithm which we call Ideal DiSP. Input  $\Omega$  and  $K$ . Output:  $\Pi_r$  and  $\Pi_c$ .

- **PCA step.** Let  $\Omega = U\Lambda V'$  be the compact SVD of  $\Omega$  such that  $U \in \mathbb{R}^{n_r \times K}$ ,  $V \in \mathbb{R}^{n_c \times K}$ ,  $\Lambda \in \mathbb{R}^{K \times K}$ ,  $U'U = I$ ,  $V'V = I$ .
- **Vertex Hunting (VH) step.** Run SP algorithm on all rows of  $U$  (and  $V$ ) assuming there are  $K$  row (column) communities to obtain  $B_r$  (and  $B_c$ ).
- **Membership Reconstruction (MR) step.** Set  $Y_r = UB_r'(B_r B_r')^{-1}$  and  $Y_c = UB_c'(B_c B_c')^{-1}$ . Recover  $\Pi_r$  and  $\Pi_c$  by setting  $\Pi_r(i, :) = \frac{Y_r(i, :)}{\|Y_r(i, :)\|_1}$  for  $1 \leq i \leq n_r$ , and  $\Pi_c(j, :) = \frac{Y_c(j, :)}{\|Y_c(j, :)\|_1}$  for  $1 \leq j \leq n_c$ .

The following theorem guarantees that Ideal DiSP exactly recover nodes memberships and this also verifies the identifiability of DiMMSB in turn.

**Theorem 1** (*Ideal DiSP*). *Under DiMMSB( $n_r, n_c, K, P, \Pi_r, \Pi_c$ ), the Ideal DiSP exactly recovers the row nodes membership matrix  $\Pi_r$  and the column nodes membership matrix  $\Pi_c$ .*

We now extend the ideal case to the real case. Set  $\tilde{A} = \hat{U}\hat{\Lambda}\hat{V}'$  be the top- $K$ -dimensional SVD of  $A$  such that  $\hat{U} \in \mathbb{R}^{n_r \times K}$ ,  $\hat{V} \in \mathbb{R}^{n_c \times K}$ ,  $\hat{\Lambda} \in \mathbb{R}^{K \times K}$ ,  $\hat{U}'\hat{U} = I_K$ ,  $\hat{V}'\hat{V} = I_K$ , and  $\hat{\Lambda}$  contains the top  $K$  singular values of  $A$ . For the real case, we use  $\hat{B}_r, \hat{B}_c, \hat{Y}_r, \hat{Y}_c, \hat{\Pi}_r, \hat{\Pi}_c$  given in Algorithm 1 to estimate  $B_r, B_c, Y_r, Y_c, \Pi_r, \Pi_c$ , respectively. Algorithm 1 called DiSP is a natural extension of the Ideal DiSP to the real case.

---

### Algorithm 1 DiSP

---

**Require:** The adjacency matrix  $A \in \mathbb{R}^{n_r \times n_c}$ , the number of row (column) communities  $K$ .

**Ensure:** The estimated  $n_r \times K$  row membership matrix  $\hat{\Pi}_r$  and the estimated  $n_c \times K$  column membership matrix  $\hat{\Pi}_c$ .

- 1: **PCA step.** Compute the left singular vectors  $\hat{U} \in \mathbb{R}^{n_r \times K}$  and right singular vectors  $\hat{V} \in \mathbb{R}^{n_c \times K}$  of  $A$ .
  - 2: **Vertex Hunting (VH) step.** Apply SP algorithm (i.e., Algorithm 4) on the rows of  $\hat{U}$  assuming there are  $K$  row clusters to obtain the near-corners matrix  $\hat{U}(\hat{\mathcal{I}}_r, :) \in \mathbb{R}^{K \times K}$ , where  $\hat{\mathcal{I}}_r$  is the index set returned by SP algorithm. Similarly, apply SP algorithm on the rows of  $\hat{V}$  with  $K$  column clusters to obtain  $\hat{V}(\hat{\mathcal{I}}_c, :) \in \mathbb{R}^{K \times K}$ , where  $\hat{\mathcal{I}}_c$  is the index set returned by SP algorithm. Set  $\hat{B}_r = \hat{U}(\hat{\mathcal{I}}_r, :)$ ,  $\hat{B}_c = \hat{V}(\hat{\mathcal{I}}_c, :)$ .
  - 3: **Membership Reconstruction (MR) step.** Compute the  $n_r \times K$  matrix  $\hat{Y}_r$  such that  $\hat{Y}_r = \hat{U}\hat{B}_r'(\hat{B}_r\hat{B}_r')^{-1}$ . Set  $\hat{Y}_r = \max(0, \hat{Y}_r)$  and estimate  $\Pi_r(i, :)$  by  $\hat{\Pi}_r(i, :) = \hat{Y}_r(i, :)/\|\hat{Y}_r(i, :)\|_1$ ,  $1 \leq i \leq n_r$ . Similarly, compute the  $n_c \times K$  matrix  $\hat{Y}_c$  such that  $\hat{Y}_c = \hat{V}\hat{B}_c'(\hat{B}_c\hat{B}_c')^{-1}$ . Set  $\hat{Y}_c = \max(0, \hat{Y}_c)$  and estimate  $\Pi_c(j, :)$  by  $\hat{\Pi}_c(j, :) = \hat{Y}_c(j, :)/\|\hat{Y}_c(j, :)\|_1$ ,  $1 \leq j \leq n_c$ .
-



In the MR step, we set the negative entries of  $\hat{Y}_r$  as 0 by setting  $\hat{Y}_r = \max(0, \hat{Y}_r)$  for the reason that weights for any row node should be nonnegative while there may exist some negative entries of  $\hat{U}\hat{B}_r'(\hat{B}_r\hat{B}_r')^{-1}$ . Meanwhile, since  $\hat{B}_r$  has  $K$  distinct rows and  $n_r$  is always much larger than  $K$ , the inverse of  $\hat{B}_r\hat{B}_r'$  always exists in practice. Similar statements hold for column nodes.

To demonstrate the RIS and CIS, we drew Figure 2. Panel (a) supports that if row node  $i$  is pure, then  $U(i, \cdot)$  falls on the vertex of the RIS, otherwise  $U(i, \cdot)$  falls in the interior of the RIS. Similar arguments hold for  $V$ . In panels (c)-(h), we plot  $\hat{U}$  and  $\hat{V}$  under different settings of the number of pure nodes in row clusters and column clusters, where the data is generated by DiMMSB under the setting of Experiment 4. And in panels (c)-(h) of Figure 2, we also plot the  $\hat{B}_r$  and  $\hat{B}_c$ . From panels (c)-(e), we can find that points in  $\hat{U}$  generated from the same row cluster are always much closer than row nodes from different row clusters. Meanwhile, as the number of pure row nodes  $n_{r,0}$  increases for each row cluster, the number of points fall in the interior of the triangle decreases. Similar arguments hold for  $\hat{V}$ .

### 3.1 Equivalence algorithm

For the convenience of theoretical analysis, we introduce an equivalent algorithm DiSP-equivalence which returns same estimations as Algorithm 1 (see Remark 7 for details). Denote  $U_2 = UU' \in \mathbb{R}^{n_r \times n_r}$ ,  $\hat{U}_2 = \hat{U}\hat{U}' \in \mathbb{R}^{n_r \times n_r}$ ,  $V_2 = VV' \in \mathbb{R}^{n_c \times n_c}$ ,  $\hat{V}_2 = \hat{V}\hat{V}' \in \mathbb{R}^{n_c \times n_c}$ . Next lemma guarantees that  $U_2$  and  $V_2$  have simplex structures.

**Lemma 2** *Under DiMMSB( $n_r, n_c, K, P, \Pi_r, \Pi_c$ ), we have  $U_2 = \Pi_r U_2(\mathcal{I}_r, \cdot)$  and  $V_2 = \Pi_c V_2(\mathcal{I}_c, \cdot)$ .*

Since  $U_2(\mathcal{I}_r, \cdot) \in \mathbb{R}^{K \times n_r}$  and  $V_2(\mathcal{I}_c, \cdot) \in \mathbb{R}^{K \times n_c}$ ,  $U_2(\mathcal{I}_r, \cdot)$  and  $V_2(\mathcal{I}_c, \cdot)$  are singular matrix with rank  $K$  by condition (I1). Lemma 2 gives that

$$\Pi_r = U_2 U_2'(\mathcal{I}_r, \cdot) (U_2(\mathcal{I}_r, \cdot) U_2'(\mathcal{I}_r, \cdot))^{-1}, \Pi_c = V_2 V_2'(\mathcal{I}_c, \cdot) (V_2(\mathcal{I}_c, \cdot) V_2'(\mathcal{I}_c, \cdot))^{-1}.$$

Based on the above analysis, we are now ready to give the Ideal DiSP-equivalence. Input  $\Omega$  and  $K$ . Output:  $\Pi_r$  and  $\Pi_c$ .

- **PCA step.** Obtain  $U_2$  and  $V_2$ .
- **VH step.** Apply SP algorithm on rows of  $U_2$  to obtain  $U_2(\mathcal{I}_r, \cdot)$  and on rows of  $V_2$  to obtain  $V_2(\mathcal{I}_c, \cdot)$  assuming there are  $K$  row (column) communities.
- **MR step.** Recover  $\Pi_r = U_2 U_2'(\mathcal{I}_r, \cdot) (U_2(\mathcal{I}_r, \cdot) U_2'(\mathcal{I}_r, \cdot))^{-1}$ ,  $\Pi_c = V_2 V_2'(\mathcal{I}_c, \cdot) (V_2(\mathcal{I}_c, \cdot) V_2'(\mathcal{I}_c, \cdot))^{-1}$ .

We now extend the ideal case to the real one as below.

Lemma 3.2 in Mao et al. (2020) gives  $\hat{\mathcal{I}}_r = \hat{\mathcal{I}}_{r,2}$  and  $\hat{\mathcal{I}}_c = \hat{\mathcal{I}}_{c,2}$  (i.e., SP algorithm will return the same indices on both  $\hat{U}$  and  $\hat{U}_2$  as well as  $\hat{V}$  and  $\hat{V}_2$ ), which gives that  $\hat{U}_2 \hat{U}_2'(\hat{\mathcal{I}}_{r,2}, \cdot) = \hat{U}_2 \hat{U}_2'(\hat{\mathcal{I}}_r, \cdot) = \hat{U} \hat{U}'(\hat{U} \hat{U}'(\hat{\mathcal{I}}_r, \cdot))' = \hat{U} \hat{U}'(\hat{U}(\hat{\mathcal{I}}_r, \cdot) \hat{U}')' = \hat{U} \hat{U}' \hat{U} \hat{U}'(\hat{\mathcal{I}}_r, \cdot) = \hat{U} \hat{U}'(\hat{\mathcal{I}}_r, \cdot)$ , and  $\hat{U}_2(\hat{\mathcal{I}}_{r,2}, \cdot) \hat{U}_2'(\hat{\mathcal{I}}_{r,2}, \cdot) = \hat{U}_2(\hat{\mathcal{I}}_r, \cdot) \hat{U}_2'(\hat{\mathcal{I}}_r, \cdot) = \hat{U}(\hat{\mathcal{I}}_r, \cdot) \hat{U}'(\hat{U}(\hat{\mathcal{I}}_r, \cdot) \hat{U}')' = \hat{U}(\hat{\mathcal{I}}_r, \cdot) \hat{U}'(\hat{\mathcal{I}}_r, \cdot)$ . Therefore,  $\hat{Y}_{r,2} = \hat{Y}_r$ ,  $\hat{\Pi}_{r,2} = \hat{\Pi}_r$ . Following similar analysis, we also have  $\hat{Y}_{c,2} = \hat{Y}_c$ , and  $\hat{\Pi}_{c,2} = \hat{\Pi}_c$ . Hence, the above analysis guarantees that the two algorithms 1 and 2 return same estimations for both row and column nodes's memberships.

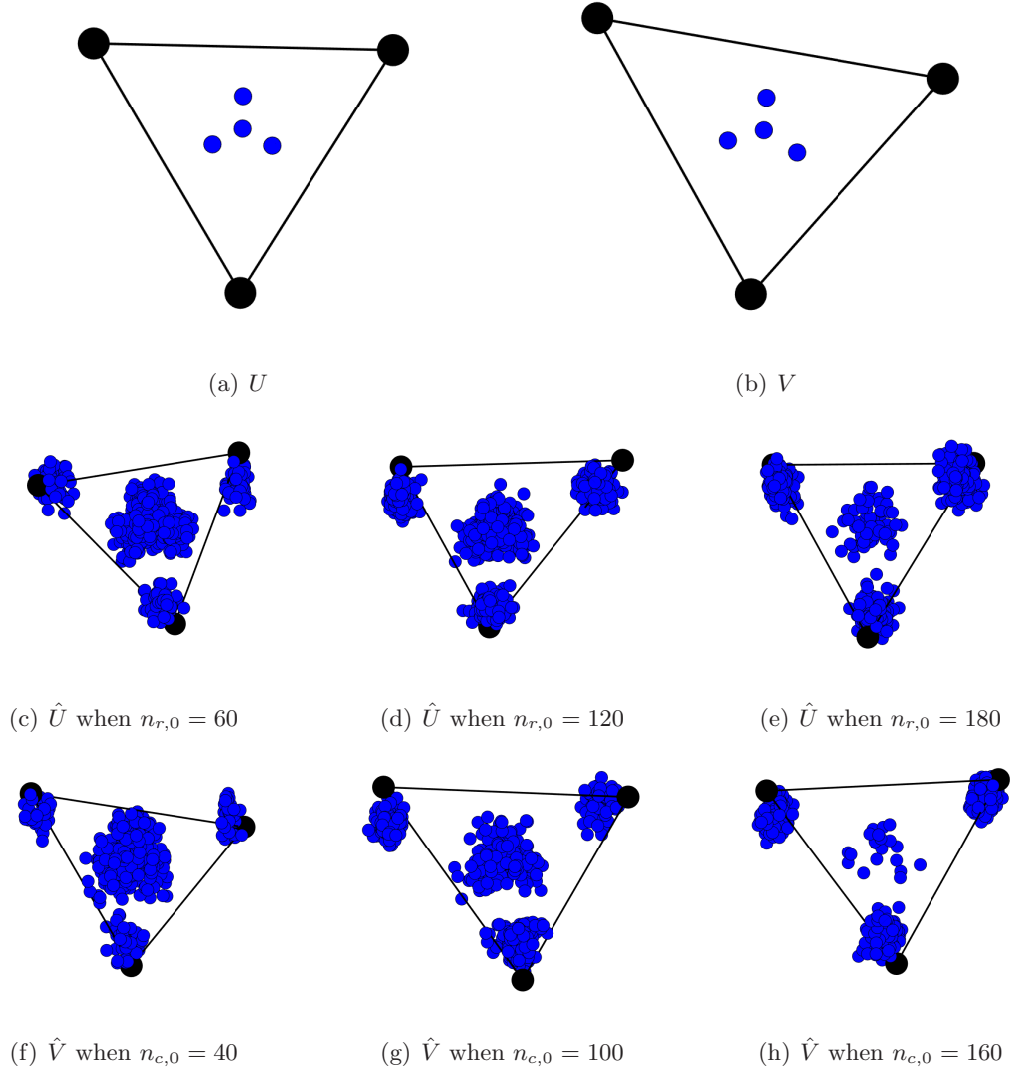


Figure 2: Panel (a) shows the RIS in Experiment 4 when  $n_{c,0} = n_{r,0} = 120$ , where  $n_{c,0}$  and  $n_{r,0}$  are the numbers of pure nodes in row and column respectively (black: pure nodes; blue: mixed nodes. Each point is a row of  $U$ . Many rows are equal, so a point may represent many rows). All mixed (both row and column) nodes evenly distributed in 4 groups, where the PMFs equal to  $(0.4, 0.4, 0.2)$ ,  $(0.4, 0.2, 0.4)$ ,  $(0.2, 0.4, 0.4)$  and  $(1/3, 1/3, 1/3)$ . Panel (b) shows the CIS with same setting as (a). Panel (c): each point is a row of  $\hat{U}$  while black point is the vertex obtained by SP algorithm in Experiment 4 when setting  $n_{r,0} = 60$ . Similar interpretations for Panels (d)-(h). Since  $K = 3$  in Experiment 4, for visualization, we have projected and rotated these points from  $\mathbb{R}^3$  to  $\mathbb{R}^2$ .

---

**Algorithm 2 DiSP-equivalence**

---

**Require:** The adjacency matrix  $A \in \mathbb{R}^{n_r \times n_c}$ , the number of row (column) communities  $K$ .

**Ensure:** The estimated  $n_r \times K$  row membership matrix  $\hat{\Pi}_{r,2}$  and the estimated  $n_c \times K$  column membership matrix  $\hat{\Pi}_{c,2}$ .

- 1: **PCA step.** Compute  $\hat{U}_2 \in \mathbb{R}^{n_r \times n_r}$  and  $\hat{V}_2 \in \mathbb{R}^{n_c \times n_c}$  of  $A$ .
  - 2: **VH step.** Apply SP algorithm on  $\hat{U}_2$  with  $K$  row clusters to obtain  $\hat{U}_2(\hat{\mathcal{I}}_{r,2}, :) \in \mathbb{R}^{K \times n_r}$  where  $\hat{\mathcal{I}}_{r,2}$  is the index set returned by SP algorithm. Similarly, apply SP algorithm on  $\hat{V}_2$  with  $K$  column clusters to obtain  $\hat{V}_2(\hat{\mathcal{I}}_{c,2}, :) \in \mathbb{R}^{K \times n_c}$  where  $\hat{\mathcal{I}}_{c,2}$  is the index set returned by SP algorithm.
  - 3: **Membership Reconstruction (MR) step.** Compute the  $n_r \times K$  matrix  $\hat{Y}_{r,2}$  such that  $\hat{Y}_{r,2} = \hat{U}_2 \hat{U}_2'(\hat{\mathcal{I}}_{r,2}, :)(\hat{U}_2(\hat{\mathcal{I}}_{r,2}, :)\hat{U}_2'(\hat{\mathcal{I}}_{r,2}, :))^{-1}$ . Set  $\hat{Y}_{r,2} = \max(0, \hat{Y}_{r,2})$  and estimate  $\Pi_{r,2}(i, :)$  by  $\hat{\Pi}_{r,2}(i, :) = \hat{Y}_{r,2}(i, :)/\|\hat{Y}_{r,2}(i, :)\|_1, 1 \leq i \leq n_r$ . Similarly, compute the  $n_c \times K$  matrix  $\hat{Y}_{c,2}$  such that  $\hat{Y}_{c,2} = \hat{V}_2 \hat{V}_2'(\hat{\mathcal{I}}_{c,2}, :)(\hat{V}_2(\hat{\mathcal{I}}_{c,2}, :)\hat{V}_2'(\hat{\mathcal{I}}_{c,2}, :))^{-1}$ . Set  $\hat{Y}_{c,2} = \max(0, \hat{Y}_{c,2})$  and estimate  $\Pi_{c,2}(j, :)$  by  $\hat{\Pi}_{c,2}(j, :) = \hat{Y}_{c,2}(j, :)/\|\hat{Y}_{c,2}(j, :)\|_1, 1 \leq j \leq n_c$ .
- 

#### 4. Main results for DiSP

In this section, we show the consistency of our algorithm, i.e., to show that the sample-based estimates  $\hat{\Pi}_r$  and  $\hat{\Pi}_c$  concentrate around the true mixed membership matrix  $\Pi_r$  and  $\Pi_c$ . Throughout this paper,  $K$  is a known positive integer.

First, we bound  $\|A - \Omega\|$  based on the application of the rectangular version of Bernstein inequality in Tropp (2012). This technique allows us to deal with rectangular random matrices, and it is the corner stone for that our algorithm DiSP can fit DiMMSB when  $n_r \neq n_c$ . We assume that

**Assumption 1**  $\rho \max(n_r, n_c) \geq \log(n_r + n_c)$ .

Assumption 1 means that the network can not be too sparse. Then we have the following lemma.

**Lemma 3** *Under DiMMSB( $n_r, n_c, K, P, \Pi_r, \Pi_c$ ), when Assumption 1 holds, with probability at least  $1 - o((n_r + n_c)^{-\alpha})$  for any  $\alpha > 0$ , we have*

$$\|A - \Omega\| = O(\sqrt{\rho \max(n_r, n_c) \log(n_r + n_c)}).$$

Then we can obtain the row-wise deviation bound for the singular eigenvectors of  $\Omega$ .

**Lemma 4** *(Row-wise singular eigenvector error) Under DiMMSB( $n_r, n_c, K, P, \Pi_r, \Pi_c$ ), when Assumption 1 holds, suppose  $\sigma_K(\Omega) \geq C \sqrt{\rho(n_r + n_c) \log(n_r + n_c)}$ , with probability at least  $1 - o((n_r + n_c)^{-\alpha})$ , we have*

$$\max(\|\hat{U}\hat{U}' - UU'\|_{2 \rightarrow \infty}, \|\hat{V}\hat{V}' - VV'\|_{2 \rightarrow \infty}) = O\left(\frac{\sqrt{K}(\kappa(\Omega) \sqrt{\frac{\max(n_r, n_c)\mu}{\min(n_r, n_c)}} + \sqrt{\log(n_r + n_c)})}{\sqrt{\rho} \sigma_K(\tilde{P}) \sigma_K(\Pi_r) \sigma_K(\Pi_c)}\right),$$

where  $\mu$  is the incoherence parameter defined as  $\mu = \max(\frac{n_r \|U\|_{2 \rightarrow \infty}^2}{K}, \frac{n_c \|V\|_{2 \rightarrow \infty}^2}{K})$ .

For convenience, set  $\varpi = \max(\|\hat{U}\hat{U}' - UU'\|_{2 \rightarrow \infty}, \|\hat{V}\hat{V}' - VV'\|_{2 \rightarrow \infty})$ . When  $n_r = n_c = n$  and  $\Pi_r = \Pi_c = \Pi$ , DiMMSB degenerates to MMSB. If we further assume that  $\lambda_K(\Pi'\Pi) = O(\frac{n}{K})$  and  $K = O(1)$ , the bound in Lemma 4 can be simplified as  $O(\frac{1}{\sigma_K(\tilde{P})} \frac{1}{\sqrt{n}} \sqrt{\frac{\log(n)}{\rho n}})$ . This simplified form is consistent with the Lemma 2.1 in Jin et al. (2017). In detail, by setting the  $\Theta$  in Jin et al. (2017) as  $\sqrt{\rho}I$  to degenerate their DCMM to MMSB, and translating their assumptions to  $\lambda_K(\Pi'\Pi) = O(\frac{n}{K})$ , when  $K = O(1)$ , the row-wise deviation bound in the fourth bullet of Lemma 2.1 in Jin et al. (2017) is the same as our reduced bound. Then if we further assume that  $\sigma_K(\tilde{P}) = O(1)$ , the bound is of order  $\frac{1}{\sqrt{n}} \sqrt{\frac{\log(n)}{\rho n}}$ , which is consistent with the row-wise eigenvector deviation of Lei (2019)'s result shown in their Table 2.

Next we bound the vertex centers matrix obtained by SP algorithm.

**Lemma 5** *Under DiMMSB( $n_r, n_c, K, P, \Pi_r, \Pi_c$ ), when conditions in Lemma 4 hold, there exist two permutation matrices  $\mathcal{P}_r, \mathcal{P}_c \in \mathbb{R}^{K \times K}$  such that with probability at least  $1 - o((n_r + n_c)^{-\alpha})$ , we have*

$$\begin{aligned} \max_{1 \leq k \leq K} \|e'_k(\hat{U}_2(\hat{\mathcal{I}}_r, \cdot) - \mathcal{P}'_r U_2(\mathcal{I}_r, \cdot))\|_F &= O(\varpi \kappa(\Pi'_r \Pi_r)), \\ \max_{1 \leq k \leq K} \|e'_k(\hat{V}_2(\hat{\mathcal{I}}_c, \cdot) - \mathcal{P}'_c V_2(\mathcal{I}_c, \cdot))\|_F &= O(\varpi \kappa(\Pi'_c \Pi_c)). \end{aligned}$$

**Lemma 6** *Under DiMMSB( $n_r, n_c, K, P, \Pi_r, \Pi_c$ ), when conditions in Lemma 4 hold, with probability at least  $1 - o((n_r + n_c)^{-\alpha})$ , for  $1 \leq i \leq n_r, 1 \leq j \leq n_c$ , we have*

$$\|e'_i(\hat{Y}_r - Y_r \mathcal{P}_r)\|_F = O(\varpi \kappa(\Pi'_r \Pi_r) \sqrt{K \lambda_1(\Pi'_r \Pi_r)}), \|e'_j(\hat{Y}_c - Y_c \mathcal{P}_c)\|_F = O(\varpi \kappa(\Pi'_c \Pi_c) \sqrt{K \lambda_1(\Pi'_c \Pi_c)}).$$

Next theorem gives theoretical bounds on estimations of memberships for both row and column nodes, which is the main theoretical result for our DiSP method.

**Theorem 2** *Under DiMMSB( $n_r, n_c, K, P, \Pi_r, \Pi_c$ ), suppose conditions in Lemma 4 hold, with probability at least  $1 - o((n_r + n_c)^{-\alpha})$ , for  $1 \leq i \leq n_r, 1 \leq j \leq n_c$ , we have*

$$\begin{aligned} \|e'_i(\hat{\Pi}_r - \Pi_r \mathcal{P}_r)\|_1 &= O(\varpi \kappa(\Pi'_r \Pi_r) K \sqrt{\lambda_1(\Pi'_r \Pi_r)}), \\ \|e'_j(\hat{\Pi}_c - \Pi_c \mathcal{P}_c)\|_1 &= O(\varpi \kappa(\Pi'_c \Pi_c) K \sqrt{\lambda_1(\Pi'_c \Pi_c)}). \end{aligned}$$

Similar as Corollary 3.1 in Mao et al. (2020), by considering more conditions, we have the following corollary.

**Corollary 1** *Under DiMMSB( $n_r, n_c, K, P, \Pi_r, \Pi_c$ ), when conditions in Lemma 4 hold, suppose  $\lambda_K(\Pi'_r \Pi_r) = O(\frac{n_r}{K})$  and  $\lambda_K(\Pi'_c \Pi_c) = O(\frac{n_c}{K})$ , with probability at least  $1 - o((n_r + n_c)^{-\alpha})$ , for  $1 \leq i \leq n_r, 1 \leq j \leq n_c$ , we have*

$$\begin{aligned} \|e'_i(\hat{\Pi}_r - \Pi_r \mathcal{P}_r)\|_1 &= O\left(\frac{K^2(\sqrt{C \frac{\max(n_r, n_c)}{\min(n_r, n_c)}} + \sqrt{\log(n_r + n_c)})}{\sigma_K(\tilde{P}) \sqrt{\rho n_c}}\right), \\ \|e'_j(\hat{\Pi}_c - \Pi_c \mathcal{P}_c)\|_1 &= O\left(\frac{K^2(\sqrt{C \frac{\max(n_r, n_c)}{\min(n_r, n_c)}} + \sqrt{\log(n_r + n_c)})}{\sigma_K(\tilde{P}) \sqrt{\rho n_r}}\right), \end{aligned}$$

where  $C$  is a positive constant. Meanwhile,

- when  $C \frac{\max(n_r, n_c)}{\min(n_r, n_c)} \leq \log(n_r + n_c)$ , we have

$$\|e'_i(\hat{\Pi}_r - \Pi_r \mathcal{P}_r)\|_1 = O\left(\frac{K^2 \sqrt{\log(n_r + n_c)}}{\sigma_K(\tilde{P}) \sqrt{\rho n_c}}\right), \|e'_j(\hat{\Pi}_c - \Pi_c \mathcal{P}_c)\|_1 = O\left(\frac{K^2 \sqrt{\log(n_r + n_c)}}{\sigma_K(\tilde{P}) \sqrt{\rho n_r}}\right).$$

- when  $n_r = O(n), n_c = O(n)$  (i.e.,  $\frac{n_r}{n_c} = O(1)$ ), we have

$$\|e'_i(\hat{\Pi}_r - \Pi_r \mathcal{P}_r)\|_1 = O\left(\frac{K^2}{\sigma_K(\tilde{P})} \sqrt{\frac{\log(n)}{\rho n}}\right), \|e'_j(\hat{\Pi}_c - \Pi_c \mathcal{P}_c)\|_1 = O\left(\frac{K^2}{\sigma_K(\tilde{P})} \sqrt{\frac{\log(n)}{\rho n}}\right).$$

Under the settings of Corollary 1, when  $K = O(1)$ , to ensure the consistency of estimation, for the case  $C \frac{\max(n_r, n_c)}{\min(n_r, n_c)} \leq \log(n_r + n_c)$ ,  $\sigma_K(\tilde{P})$  should shrink slower than  $\sqrt{\frac{\log(n_r + n_c)}{\rho \min(n_r, n_c)}}$ ; Similarly, for the case  $\frac{n_r}{n_c} = O(1)$ ,  $\sigma_K(\tilde{P})$  should shrink slower than  $\sqrt{\frac{\log(n)}{\rho n}}$ .

**Remark 1** By Lemma 10, we know  $\sigma_K(\Omega) \geq \rho \sigma_K(\tilde{P}) \sigma_K(\Pi_r) \sigma_K(\Pi_c)$ . To ensure the condition  $\sigma_K(\Omega) \geq C(\rho(n_r + n_c) \log(n_r + n_c))^{1/2}$  in lemma 4 hold, we need  $\rho \sigma_K(\tilde{P}) \sigma_K(\Pi_r) \sigma_K(\Pi_c) \geq C(\rho(n_r + n_c) \log(n_r + n_c))^{1/2}$ . Thus

$$\sigma_K(\tilde{P}) \geq C \left( \frac{(n_r + n_c) \log(n_r + n_c)}{\rho \lambda_K(\Pi'_r \Pi_r) \lambda_K(\Pi'_c \Pi_c)} \right)^{1/2}. \quad (8)$$

When  $K = O(1)$ ,  $\lambda_K(\Pi'_r \Pi_r) = O(\frac{n_r}{K})$ , and  $\lambda_K(\Pi'_c \Pi_c) = O(\frac{n_c}{K})$ , Eq (8) gives that  $\sigma_K(\tilde{P})$  should grow faster than  $\log^{1/2}(n_r + n_c) / (\rho \min(n_r, n_c))^{1/2}$ , which matches with the consistency requirement on  $\sigma_K(\tilde{P})$  obtained from Corollary 1.

**Remark 2** When DiMMSB degenerates to MMSB, for the network with  $n_r = n_c = n$  and  $K = O(1)$ , the upper bound of error rate for DiSP is  $O(\frac{1}{\sigma_K(\tilde{P})} \sqrt{\frac{\log(n)}{\rho n}})$ . Replacing the  $\Theta$  in Jin et al. (2017) by  $\Theta = \sqrt{\rho} I$ , their DCMM model degenerates to the MMSB. Then their conditions in Theorem 2.2 are the same as our assumption (1) and  $\lambda_K(\Pi' \Pi) = O(\frac{n}{K})$  where  $\Pi = \Pi_r = \Pi_c$  for MMSB. When  $K = O(1)$ , the error bound in Theorem 2.2 in Jin et al. (2017) is  $O(\frac{1}{|\lambda_K(\tilde{P})|} \sqrt{\frac{\log(n)}{\rho n}})$ , which is consistent with ours since  $|\lambda_K(\tilde{P})| = \sigma_K(\tilde{P})$ . This guarantees the optimality of our theoretical results.

Similarly, under the settings of Corollary 1, for the case  $C \frac{\max(n_r, n_c)}{\min(n_r, n_c)} \leq \log(n_r + n_c)$ , when  $\sigma_K(\tilde{P})$  is a constant, the upper bounds of error rates for both row clusters and column clusters are  $O(K^2 \sqrt{\frac{\log(n_r + n_c)}{\rho \min(n_r, n_c)}})$ . Therefore, for consistent estimation of DiSP,  $K$  should grow slower than  $(\frac{\rho \min(n_r, n_c)}{\log(n_r + n_c)})^{1/4}$ . Similarly, under the settings of Corollary 1, for the case  $\frac{n_r}{n_c} = O(1)$ , when  $\sigma_K(\tilde{P})$  is a constant, the upper bounds of error rates are  $O(K^2 \sqrt{\frac{\log(n)}{\rho n}})$ . For consistent estimation,  $K$  should grow slower than  $(\frac{\rho n}{\log(n)})^{1/4}$ .

Consider the balanced directed mixed membership network (i.e.,  $\lambda_K(\Pi'_r \Pi_r) = O(\frac{n_r}{K})$ ,  $\lambda_K(\Pi'_c \Pi_c) = O(\frac{n_c}{K})$  and  $n_r = O(n), n_c = O(n)$ ) in Corollary 1, we further assume that  $\tilde{P} = \beta I_K + (1 - \beta) \mathbf{1}_K \mathbf{1}'_K$  (where  $\mathbf{1}_K$  is a  $K \times 1$  vector with all entries being ones.) for  $0 < \beta < 1$  when

$K = O(1)$  and call such directed network as standard directed mixed membership network. To obtain consistency estimation,  $\beta$  should shrink slower than  $\sqrt{\frac{\log(n)}{\rho n}}$  since  $\sigma_K(\tilde{P}) = \beta$ . Let  $P_{\max} = \max_{k,l} P(k, l)$ ,  $P_{\min} = \min_{k,l} P(k, l)$ . Since  $P = \rho\tilde{P}$ , we have  $P_{\max} - P_{\min} = \rho\beta$  (the probability gap) should shrink slower than  $\sqrt{\frac{\rho\log(n)}{n}}$  and  $\frac{P_{\max} - P_{\min}}{\sqrt{P_{\max}}} = \beta\sqrt{\rho}$  (the relative edge probability gap) should shrink slower than  $\sqrt{\frac{\log(n)}{n}}$ . Especially, for the sparsest network  $\rho n = \log(n)$  satisfying assumption (1), the probability gap should shrink slower than  $\frac{\log(n)}{n}$ .

## 5. Simulations

In this section, some simulations are conducted to investigate the performance of our DiSP. We measure the performance of the proposed method by Di-Mixed-Hamming error rate, row-Mixed-Hamming error rate and column-Mixed-Hamming error rate, and they are defined as:

- DiMHamm =  $\frac{\min_{\mathcal{P} \in \mathcal{S}} \|\hat{\Pi}_r \mathcal{P} - \Pi_r\|_1 + \min_{\mathcal{P} \in \mathcal{S}} \|\hat{\Pi}_c \mathcal{P} \Pi_c\|_1}{n_r + n_c}$ ,
- row-MHamm =  $\frac{\min_{\mathcal{P} \in \mathcal{S}} \|\hat{\Pi}_r \mathcal{P} - \Pi_r\|_1}{n_r}$ ,
- column-MHamm =  $\frac{\min_{\mathcal{P} \in \mathcal{S}} \|\hat{\Pi}_c \mathcal{P} - \Pi_c\|_1}{n_c}$ ,

where  $\Pi_r$  ( $\Pi_c$ ) and  $\hat{\Pi}_r$  ( $\hat{\Pi}_c$ ) are the true and estimated row (column) mixed membership matrices respectively, and  $\mathcal{S}$  is the set of  $K \times K$  permutation matrices. Here, we also consider the permutation of labels since the measurement of error should not depend on how we label each of the  $K$  communities. DiMHamm is used to measure the DiSP's performances on both row nodes and column nodes, while row-MHamm and column-MHamm are used to measure its performance on row nodes and column nodes respectively. Meanwhile, in the following 1-3 experiments, we compare DiSP with the variational expectation-maximization (vEM for short) algorithm Airoidi et al. (2013) for their two-way stochastic blockmodels with Bernoulli distribution. By Table 1 in Airoidi et al. (2013), we see that vEM under the two input Dirichlet parameters  $\alpha = 0.05, \beta = 0.05$  (by Airoidi et al. (2013)'s notation) generally performs better than that under  $\alpha = \beta = 0.2$ . Therefore, in our simulations, we set the two Dirichlet parameters  $\alpha$  and  $\beta$  of vEM as 0.05.

For the first three simulations in this section, unless specified, the parameters  $(n_r, n_c, K, P, \Pi_r, \Pi_c)$  under DiMMSB are set as follows. For row nodes,  $n_r = 60$  and  $K = 3$ . Let each row block own  $n_{r,0}$  number of pure nodes. We let the top  $Kn_{r,0}$  row nodes  $\{1, 2, \dots, Kn_{r,0}\}$  be pure and the rest row nodes  $\{Kn_{r,0} + 1, Kn_{r,0} + 2, \dots, n_r\}$  be mixed. Unless specified, let all the mixed row nodes have four different memberships  $(0.4, 0.4, 0.2)$ ,  $(0.4, 0.2, 0.4)$ ,  $(0.2, 0.4, 0.4)$  and  $(1/3, 1/3, 1/3)$ , each with  $\frac{n_r - Kn_{r,0}}{4}$  number of nodes when  $K = 3$ . For column nodes, set  $n_c = 80$ . Let each column block own  $n_{c,0}$  number of pure nodes. Let the top  $Kn_{c,0}$  column nodes  $\{1, 2, \dots, Kn_{c,0}\}$  be pure and column nodes  $\{Kn_{c,0} + 1, Kn_{c,0} + 2, \dots, n_c\}$  be mixed. The settings of column mixed memberships are same as row mixed memberships. When  $n_{r,0} = n_{c,0}$ , denote  $n_0 = n_{r,0} = n_{c,0}$  for convenience. The probability matrix  $P$  is set independently for each experiment.



After obtaining  $P, \Pi_r, \Pi_c$ , similar as the five simulation steps in Jin (2015), each simulation experiment contains the following steps:

(a) Set  $\Omega = \Pi_r P \Pi_c'$ .

(b) Let  $W$  be an  $n_r \times n_c$  matrix such that  $W(i, j)$  are independent centered-Bernoulli with parameters  $\Omega(i, j)$ . Let  $\tilde{A} = \Omega + W$ .

(c) Set  $\tilde{S}_r = \{i : \sum_{j=1}^{n_c} \tilde{A}(i, j) = 0\}$  and  $\tilde{S}_c = \{j : \sum_{i=1}^{n_r} \tilde{A}(i, j) = 0\}$ , i.e.,  $\tilde{S}_r$  ( $\tilde{S}_c$ ) is the set of row (column) nodes with 0 edges. Let  $A$  be the adjacency matrix obtained by removing rows respective to nodes in  $\tilde{S}_r$  and removing columns respective to nodes in  $\tilde{S}_c$  from  $\tilde{A}$ . Similarly, update  $\Pi_r$  by removing nodes in  $\tilde{S}_r$  and update  $\Pi_c$  by removing nodes in  $\tilde{S}_c$ .

(d) Apply DiSP (and vEM) algorithm to  $A$ . Record DiMHamm, row-MHamm, column-MHamm and running time under investigations.

(e) Repeat (b)-(d) for 50 times, and report the averaged DiMHamm, averaged row-MHamm, averaged column-MHamm and averaged running time over the 50 repetitions.

In our experiments, the number of rows of  $A$  and the number of columns of  $A$  are usually very close to  $n_r$  and  $n_c$ , therefore we do not report the exact values of the the number of rows and columns of  $A$ .

**Experiment 1: Changing  $n_0$ .** The probability matrix in this experiment is set as

$$P = \begin{bmatrix} 0.8 & 0.1 & 0.3 \\ 0.2 & 0.9 & 0.4 \\ 0.5 & 0.2 & 0.9 \end{bmatrix}.$$

Let  $n_0$  range in  $\{4, 8, 12, 16, 20\}$ . A larger  $n_0$  indicates a case with higher fraction of pure nodes for both row clusters and column clusters. The numerical results of error rates are shown in Panels (a), (b) and (c) of Figure 3. From the three panels, we see that the three error rates look similar, and the fraction of pure nodes influences the performance of DiSP and vEM such that the two methods perform better with the increasing number of pure nodes in the simulated network. The plots of run-time are shown in panel (j) of Figure 3. Meanwhile, codes for all numerical results in this paper are written in MATLAB R2021b. The total run-time of Experiment 1 for vEM is roughly 8 hours, and it is roughly 1.5 seconds for DiSP. Sure, DiSP outperforms vEM on both error rates and run-time.

**Experiment 2: Changing  $\rho$ .** Let the sparsity parameter  $\rho \in \{0.1, 0.2, \dots, 1\}$ . The probability matrix in this experiment is set as

$$P = \rho \begin{bmatrix} 1 & 0.4 & 0.4 \\ 0.6 & 1 & 1 \\ 0.2 & 0.2 & 0.4 \end{bmatrix}.$$

A larger  $\rho$  indicates a denser simulated network. Here,  $P$  is set much different as that in Experiment 1, because we aim to emphasize that DiMMSB has no strict constraints on  $P$  as long as  $\text{rank}(P) = K$  and all elements of  $P$  are in  $[0, 1]$ . Panels (d), (e) and (f) in Figure 3 display simulation results of this experiment and panel (k) records run-time. Meanwhile, the total run-time of Experiment 2 for vEM is roughly 16 hours, and it is roughly 3.44 seconds for DiSP. From these results, we see that DiSP outperforms vEM on DiMHamm, column-MHamm and run-time while vEM performs better than DiSP on row-MHamm.

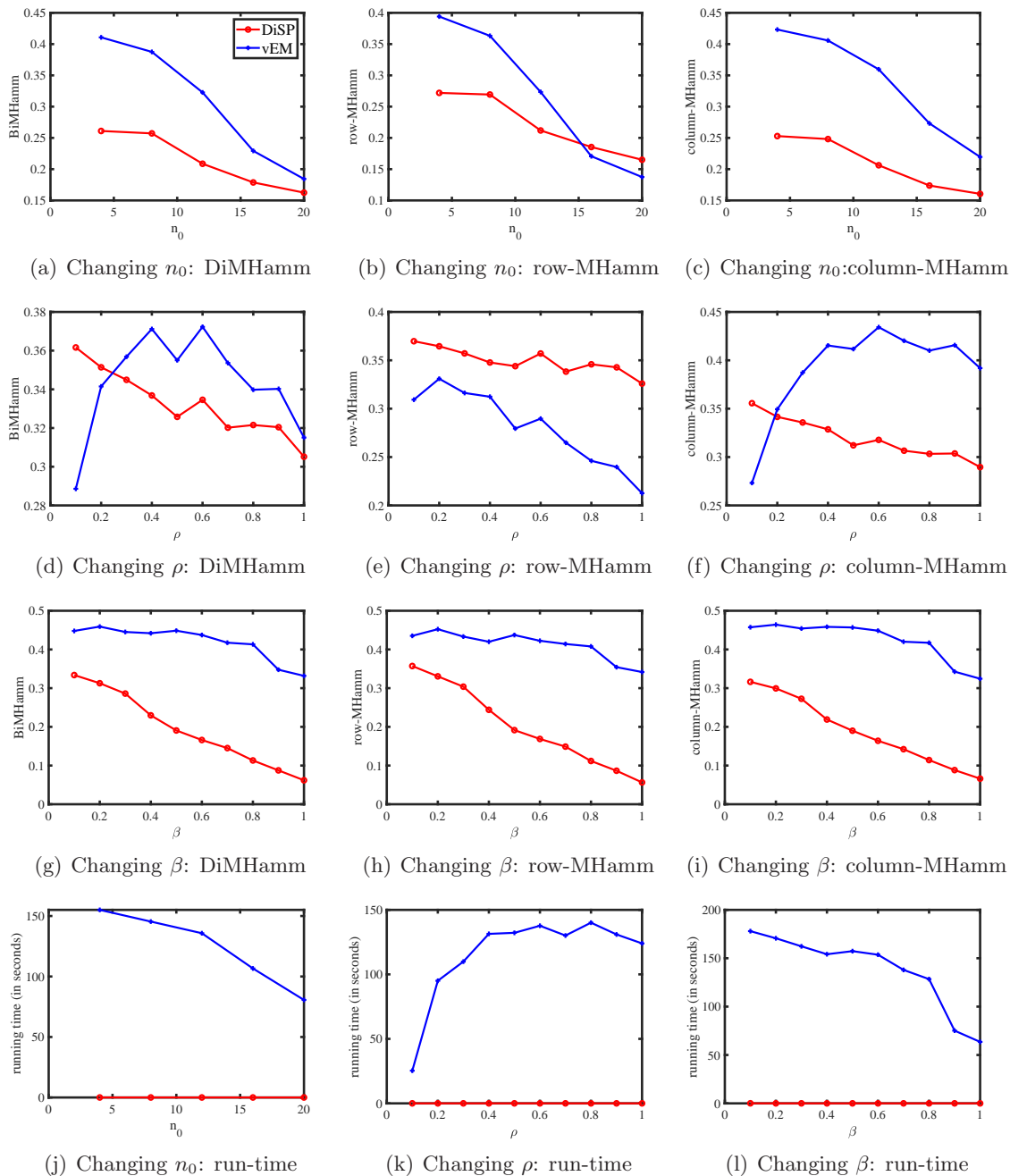


Figure 3: Numerical results of Experiments 1-3.

**Experiment 3: Changing  $\beta$ .** Let  $\beta \in \{0.1, 0.2, \dots, 1\}$ . The probability matrix in this experiment is set as

$$P = \begin{bmatrix} 1 & 1 - \beta & 1 - \beta \\ 1 - \beta & 1 & 1 - \beta \\ 1 - \beta & 1 - \beta & 1 \end{bmatrix}.$$

Since  $\sigma_K(P) = \beta$ , increasing  $\beta$  decreases error rates by the analysis for the balanced directed mixed membership network. Panels (g), (h) and (i) in Figure 3 display simulation results of this experiment and panel (l) records run-time. These three error rates are similar in this experiment. Meanwhile, the total run-time of Experiment 2 for vEM is roughly 16 hours, and it is roughly 2.9 seconds for DiSP. We see that, DiSP outperforms vEM on both error rates and run-time.

**Remark 3** For visuality, we plot  $A$  generated under DiMMSB. Let  $n_r = 24, n_c = 30, K = 2$ , and

$$P = \begin{bmatrix} 0.8 & 0.05 \\ 0.1 & 0.7 \end{bmatrix}.$$

For row nodes, let  $\Pi_r(i, 1) = 1$  for  $1 \leq i \leq 8$ ,  $\Pi_r(i, 2) = 1$  for  $9 \leq i \leq 16$ , and  $\Pi_r(i, :) = [0.7 \ 0.3]$  for  $17 \leq i \leq 24$  (i.e., there are 16 pure row nodes and 8 mixed row nodes). For column nodes, let  $\Pi_c(i, 1) = 1$  for  $1 \leq i \leq 8$ ,  $\Pi_c(i, 2) = 1$  for  $9 \leq i \leq 16$ , and  $\Pi_c(i, :) = [0.7 \ 0.3]$  for  $17 \leq i \leq 30$  (i.e., there are 16 pure column nodes and 14 mixed column nodes). For above setting, we generate two random adjacency matrices in Figure 4 where we also report error rates and run-time of DiSP and vEM. Here, because  $A$  is provided in Figure 4, and  $\Pi_r, \Pi_c$  and  $K$  are known, readers can apply DiSP to  $A$  in Figure 4 to check the effectiveness of the proposed algorithm.

**Remark 4** For visuality, we also plot a directed network generated under DiMMSB. Let  $n_r = 24, n_c = 24, K = 2$ , and

$$P = 0.8 \begin{bmatrix} 1 & 0.1 \\ 0.2 & 0.6 \end{bmatrix}.$$

For row nodes, let  $\Pi_r(i, 1) = 1$  for  $1 \leq i \leq 8$ ,  $\Pi_r(i, 2) = 1$  for  $9 \leq i \leq 16$ , and  $\Pi_r(i, :) = [0.7 \ 0.3]$  for  $17 \leq i \leq 24$  (i.e., there are 16 pure row nodes and 8 mixed row nodes). For column nodes, let  $\Pi_c(i, 1) = 1$  for  $1 \leq i \leq 10$ ,  $\Pi_c(i, 2) = 1$  for  $11 \leq i \leq 20$ , and  $\Pi_c(i, :) = [0.7 \ 0.3]$  for  $21 \leq i \leq 24$  (i.e., there are 20 pure column nodes and 4 mixed column nodes). For above setting, we generate one  $A$  in panel (a) and (b) of Figure 5 and panels (b) and (c) of Figure 5 show the sending pattern side and receiving pattern side of this simulated directed network, respectively.

In Experiments 1-3, we mainly investigate the performances of DiSP by comparing it with vEM on small directed mixed membership networks. The numerical results show that DiSP performs much better than vEM on error rates, and DiSP is much faster than vEM. However, the error rates are always quite large in Experiments 1-3 because the directed mixed membership network with 60 row nodes and 80 column nodes is too small and a few edges can be generated for such small directed mixed membership network under the settings in Experiments 1-3. In next four experiments, we investigate the performances of DiSP on some larger (compared with those under Experiments 1-3) directed mixed membership

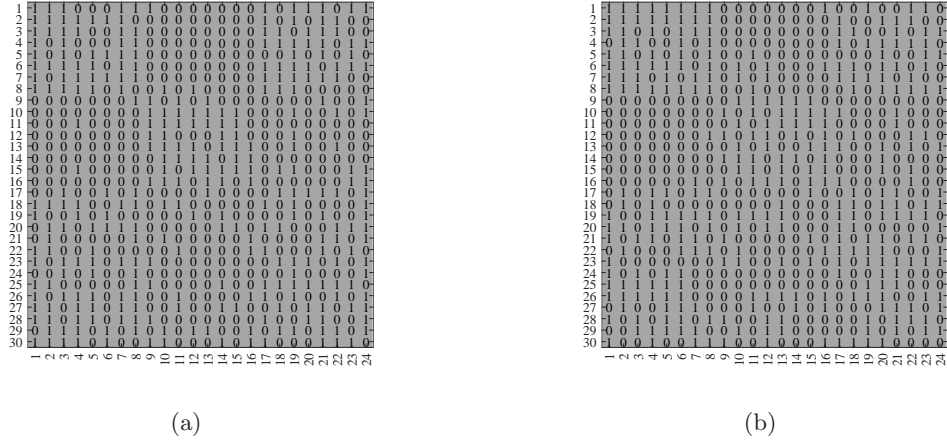


Figure 4: For adjacency matrix in panel (a), DiMHamm, row – MHamm, column – MHamm and run-time for DiSP (vEM) are 0.0948 (0.1674),0.1070 (0.1384), 0.0849 (0.0948) and 0.0021(3.7988), respectively. For adjacency matrix in panel (b), DiMHamm, row – MHamm, column – MHamm and run-time for DiSP (vEM) are 0.0778 (0.1745),0.0643 (0.1290), 0.0886 (0.2109) and 0.0020 (5.3025) seconds, respectively. x-axis: row nodes; y-axis: column nodes.

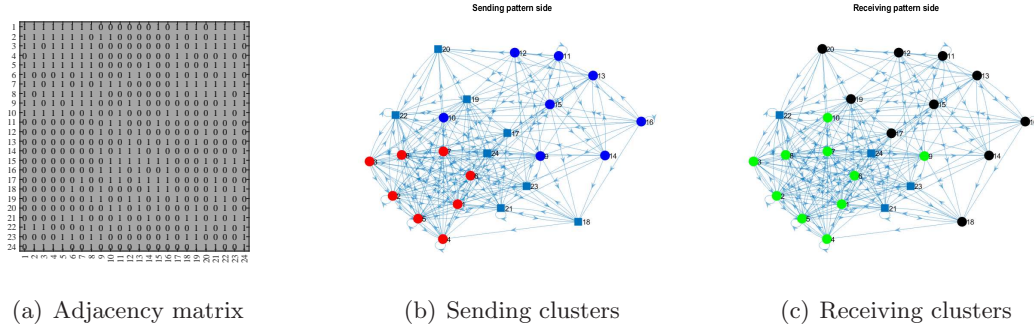


Figure 5: Illustration of a simulated directed network generated under DiMMSB. Panels (a), (b) and (c) show  $A$ , the sending clusters and the receiving clusters of this simulated directed network, respectively. For this directed network, DiMHamm, row – MHamm, column – MHamm and run-time for DiSP (vEM) are 0.0796 (0.0956),0.0786 (0.1340), 0.0806 (0.0572) and 0.0021 (2.5566) seconds, respectively. In panels (b) and (c), colors indicate clusters and square indicates mixed nodes, where the sending and receiving clusters are obtained by  $\Pi_r$  and  $\Pi_c$  given in Remark 4. x-axis: row nodes; y-axis: column nodes.

networks. Because the run-time for vEM is too large for large network, we do not compare DiSP with vEM in next four experiments.

**Experiment 4: Changing  $n_0$ .** Let  $n_r = 600, n_c = 800, n_0$  range in  $\{40, 60, \dots, 200\}$ , and all other parameters are set the same as Experiment 1. Panels (a), (b) and (c) of Figure 6 record the error rates of DiSP in Experiment 4, and panel (m) records the run-time. The total run-time for Experiment 4 is roughly 36 seconds. We see that as the fraction of pure nodes increases, error rates decreases. Meanwhile, since size of network is much larger than network in Experiment 1, error rates in Experiment 4 are much smaller than that of Experiment 1 (similar conclusions hold for Experiments 5-6).

**Experiment 5: Changing  $\rho$ .** Let  $n_r = 600, n_c = 800, n_0 = 120$  and all other parameters are set the same as Experiment 2. Panels (d), (e) and (f) of Figure 6 record the error rates of DiSP in Experiment 5, and panel (n) records the run-time. The total run-time for Experiment 5 is roughly 55 seconds. We see that as  $\rho$  increases, error rates tends to decrease.

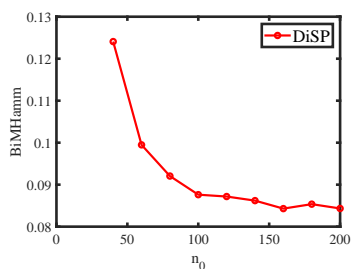
**Experiment 6: Changing  $\beta$ .** Let  $n_r = 600, n_c = 800, n_0 = 120$  and all other parameters are set the same as Experiment 3. Panels (g), (h) and (i) of Figure 6 record the error rates of DiSP in Experiment 6, and panel (o) records the run-time. The total run-time for Experiment 6 is roughly 40.6 seconds. We see that as  $\beta$  increases, error rates decreases, and this is consistent with the theoretical results in the last paragraph of Section 4.

**Experiment 7: Changing  $K$ .** Let  $n_r = 1200, n_c = 1600, n_0 = 120$ . Set diagonal elements, upper triangular elements and lower triangular elements of  $P$  as 0.5, 0.2, 0.3, respectively.  $K$  is varied in the range  $\{2, 3, \dots, 8\}$ . For the  $n_r - Kn_0$  mixed row nodes and the  $n_c - Kn_0$  mixed column nodes, let them belong to each block with equal probability  $\frac{1}{K}$ . Panels (j), (k) and (l) of Figure 6 record the error rates of DiSP in Experiment 7, and panel (p) records the run-time. The total run-time for Experiment 7 is roughly 407 seconds. From the numerical results, we see that as  $K$  increases, error rates increases first and then decreases. This phenomenon occurs since  $n_r$  and  $n_c$  are fixed, for a small  $K$ , the fraction of pure row (column) nodes  $\frac{120K}{1200}$  ( $\frac{120K}{1600}$  for column node) is small while the fraction of mixed row (column) nodes is large. As  $K$  increases in this experiment, the fraction of pure row (column) nodes increases, and this is the reason that the proposed method performs better as  $K$  increases when  $K \geq 6$ .

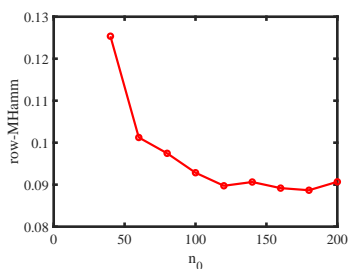
## 6. Applications to real-world data sets

For real-world directed networks considered in this paper, row nodes are always same as column nodes, so we have  $n_r = n_c = n$ . Set  $d_r(i) = \sum_{j=1}^n A(i, j)$  as the sending side degree of node  $i$ , and  $d_c(i) = \sum_{j=1}^n A(j, i)$  as the receiving side degree of node  $i$ . We find that there exist many nodes with zero degree in real-world directed networks. Before applying our DiSP on adjacency matrix of real-world directed network, we need to pre-process the original directed network by Algorithm 3.

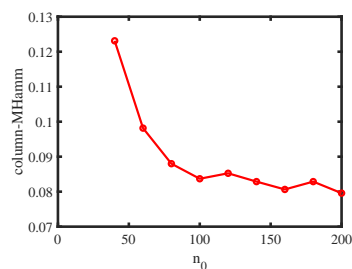
After pre-processing, we let  $\hat{\Pi}_r$  and  $\hat{\Pi}_c$  obtained from applying DiSP on  $A$  with  $n$  nodes and  $K$  row (column) communities. Let  $\hat{\ell}_r$  be an  $n \times 1$  vector such that  $\hat{\ell}_r(i) = \operatorname{argmax}_{1 \leq k \leq K} \hat{\Pi}_r(i, k)$ , where  $\hat{\ell}_r(i)$  is called the home base row community of node  $i$ .  $\hat{\ell}_c$  is defined similarly by setting  $\hat{\ell}_c(i) = \operatorname{argmax}_{1 \leq k \leq K} \hat{\Pi}_c(i, k)$ . We also need below statistics to investigate the directed network.



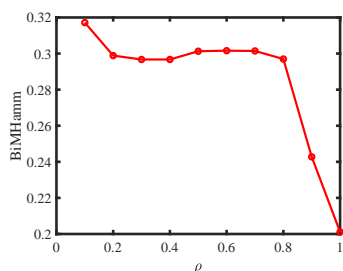
(a) Changing  $n_0$ : DiMHamm



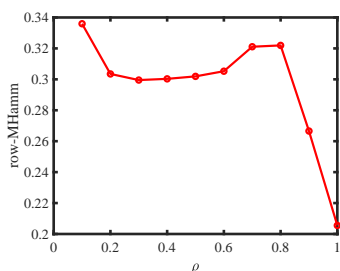
(b) Changing  $n_0$ : row-MHamm



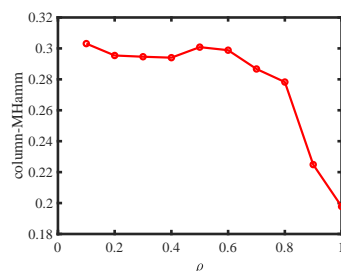
(c) Changing  $n_0$ : column-MHamm



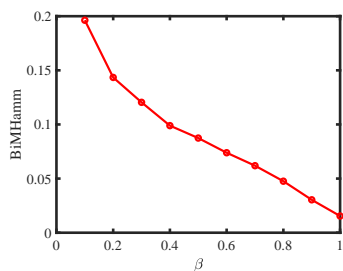
(d) Changing  $\rho$ : DiMHamm



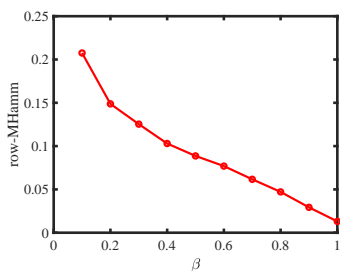
(e) Changing  $\rho$ : row-MHamm



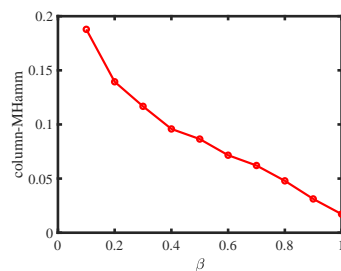
(f) Changing  $\rho$ : column-MHamm



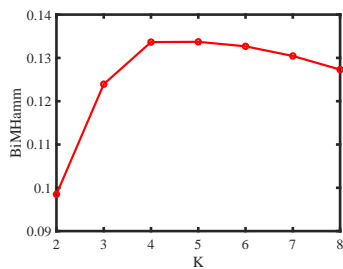
(g) Changing  $\beta$ : DiMHamm



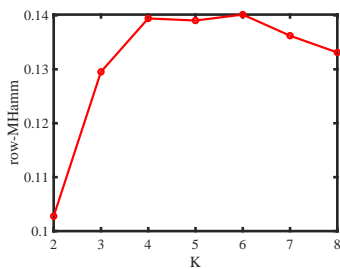
(h) Changing  $\beta$ : row-MHamm



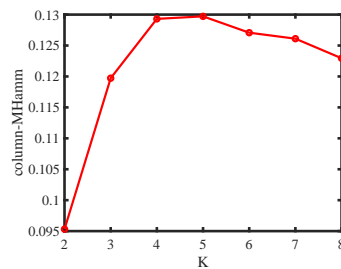
(i) Changing  $\beta$ : column-MHamm



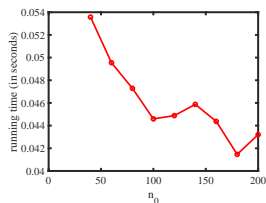
(j) Changing  $K$ : DiMHamm



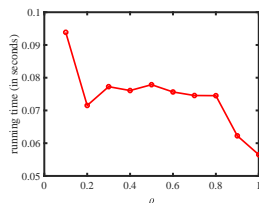
(k) Changing  $K$ : row-MHamm



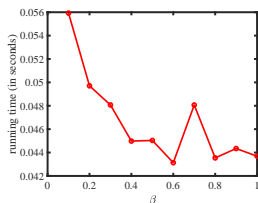
(l) Changing  $K$ : column-MHamm



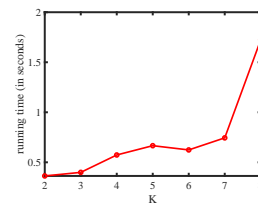
(m) Changing  $n_0$ : run-time



(n) Changing  $\rho$ : run-time



(o) Changing  $\beta$ : run-time



(p) Changing  $K$ : run-time

Figure 6: Numerical results of Experiments 4-7.



---

**Algorithm 3** Pre-processing

---

**Require:** Real-world directed network  $\mathcal{N}$ .

- 1: Set  $A_0$  as the adjacency matrix of the original directed network  $\mathcal{N}$ .
  - 2: Find the row nodes set in which row nodes have zero degree by setting  $S_{r,0} = \{i : \sum_{j=1}^n A_0(i,j) = 0\}$ . For column nodes, set  $S_{c,0} = \{i : \sum_{j=1}^n A_0(j,i) = 0\}$ .
  - 3: Set  $S_0 = S_{r,0} \cup S_{c,0}$
  - 4: Update  $A_0$  by setting  $A_0 = A_0(S_0, S_0)$ .
  - 5: Repeat step 1 and step 2 until all nodes in  $S_0$  is null set.
  - 6: Set  $A$  as the largest connected component of  $A_0$ .
- 

- **Fraction of estimated highly mixed row (column) nodes:** For row node  $i$ , we treat it as a highly mixed row node if  $\max_{1 \leq k \leq K} \hat{\Pi}(i, k) \leq 0.8$ . Let  $\tau_r$  be the proportion of highly mixed row nodes such that  $\tau_r = \frac{|\{i: \max_{1 \leq k \leq K} \hat{\Pi}_r(i, k) \leq 0.8\}|}{n}$ . Let  $\tau_c$  be the proportion of highly mixed column nodes such that  $\tau_c = \frac{|\{i: \max_{1 \leq k \leq K} \hat{\Pi}_c(i, k) \leq 0.8\}|}{n}$ .
- **The measurement of asymmetric structure between row clusters and column clusters:** Since row nodes and column nodes are the same, to see whether the structure of row clusters differs from the structure of column clusters, we use the mixed-Hamming error rate computed as

$$\text{MHamm} = \frac{\min_{O \in \mathcal{S}} \|\hat{\Pi}_r O - \hat{\Pi}_c\|_1}{n}.$$

We see that a larger (or a smaller) MHamm indicates a heavy (slight) asymmetric between row communities and column communities.

We are now ready to describe some real-world directed networks as below:

**Political blogs:** this data was collected at 2004 US presidential election Adamic and Glance (2005). Such political blogs data can be represented by a directed graph, in which each node in the graph corresponds to a web blog labelled either as liberal or conservative (i.e.,  $K = 2$  for this data). An directed edge from node  $i$  to node  $j$  indicates that there is a hyperlink from blog  $i$  to blog  $j$ . Clearly, such a political blog graph is directed due to the fact that there is a hyperlink from blog  $i$  to  $j$  does not imply there is also a hyperlink from blog  $j$  to  $i$ . This data can be downloaded from <http://www-personal.umich.edu/~mejn/netdata/>. The original data has 1490 nodes, after pre-processing by Algorithm 3,  $A \in \{0, 1\}^{813, 813}$ .

**Human proteins (Stelzl):** this network can be downloaded from <http://konect.cc/networks/maayan-Stelzl> and it represents interacting pairs of protein in Humans (*Homo sapiens*) Stelzl et al. (2005). In this data, node means protein and edge means interaction. The original data has 1706 nodes, after pre-processing,  $A \in \{0, 1\}^{1507 \times 1507}$ . The number of row (column) clusters is unknown, to estimate it, we plot the leading 20 singular values of  $A$  in panel (b) of Figure 7 and find that the eigengap suggests  $K = 2$ . Meanwhile, Rohe et al. (2016) also uses the idea of eigengap to choose  $K$  for directed networks.

**Wikipedia links (crh):** this data represents the wikilinks of the Wikipedia in the Crimean Turkish language (crh), and it can be downloaded from [http://konect.cc/networks/wikipedia\\_link\\_crh/](http://konect.cc/networks/wikipedia_link_crh/). In this network, node denotes article, and edge denotes wikilink Kunegis (2013). After pre-processing, there are 3555 nodes, i.e.,  $A \in \{0, 1\}^{3555 \times 3555}$ . Panel (c) of Figure 7 suggests

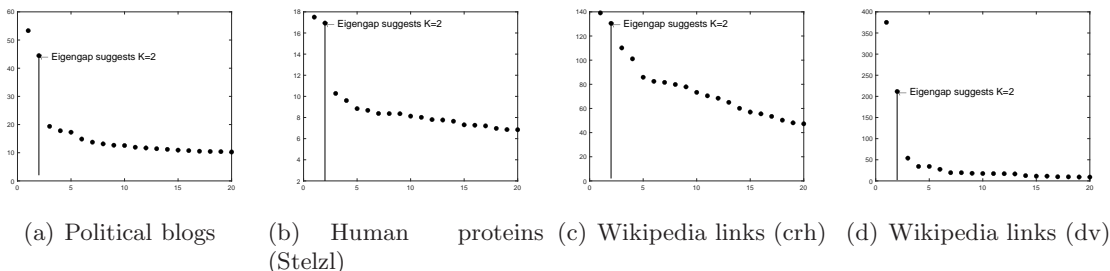


Figure 7: Leading 20 singular values of adjacency matrices for real world directed networks used in this paper.

$K = 2$  for this data.

**Wikipedia links (dv):** this data consists of the wikilinks of the Wikipedia in the Divehi language (dv) where nodes are Wikipedia articles, and directed edges are wikilinks Kunegis (2013). It can be downloaded from [http://konect.cc/networks/wikipedia\\_link\\_dv/](http://konect.cc/networks/wikipedia_link_dv/). After pre-processing,  $A \in \{0, 1\}^{2394 \times 2394}$ .  $K = 2$  for this data. Panel (d) of Figure 7 suggests  $K = 2$  for this data.

After obtaining  $A$  and  $K$  for real-world directed networks analyzed in this paper, we apply our DiSP to  $A$ , and report  $\tau_r, \tau_c$  and MHamm in Table 1. The results show that there is a slight asymmetric structure between row and column clusters for Political blogs, Human proteins (Stelzl) and Wikipedia links (crh) networks, because their MHamm is small, while row clusters differs a lot from column clusters for Wikipedia links (dv) for its large MHamm. For Political blogs, there exist  $813 \times 0.0246 \approx 20$  highly mixed nodes in the sending pattern side while there exist  $813 \times 0.1353 \approx 110$  highly mixed nodes in the receiving pattern side. For Human proteins (Stelzl), it has  $1507 \times 0.2986 \approx 450$  (and  $1507 \times 0.2999 \approx 452$ ) highly mixed nodes in the sending (receiving) pattern side. For Wikipedia links (crh), there are  $3555 \times 0.0444 \approx 158$  (and  $3555 \times 0.1308 \approx 465$ ) highly mixed nodes in the sending (receiving) pattern side. For Wikipedia links (dv), it has a large proportion of highly mixed nodes in both sending and receiving pattern side. Meanwhile, for visualization, we plot the sending clusters and receiving clusters detected by DiSP for real-world directed networks used in this paper in Figure 8, where we also mark the highly mixed nodes by square. Generally, we see that DiSP is useful in finding the highly mixed nodes and studying the asymmetric structure between row and column clusters of a directed network.

## 7. Discussions

In this paper, we introduce a directed mixed membership stochastic blockmodel to model directed network with mixed memberships. DiMMSB allows that both row and column nodes have mixed memberships, but the numbers of row nodes and column nodes could be different. We propose a spectral algorithm DiSP based on the SVD, SP algorithm and membership reconstruction skills. The theoretical results of DiSP show that DiSP can consistently recover memberships of both row nodes and column nodes under mild conditions. Meanwhile, we also obtain the separation conditions of a standard directed

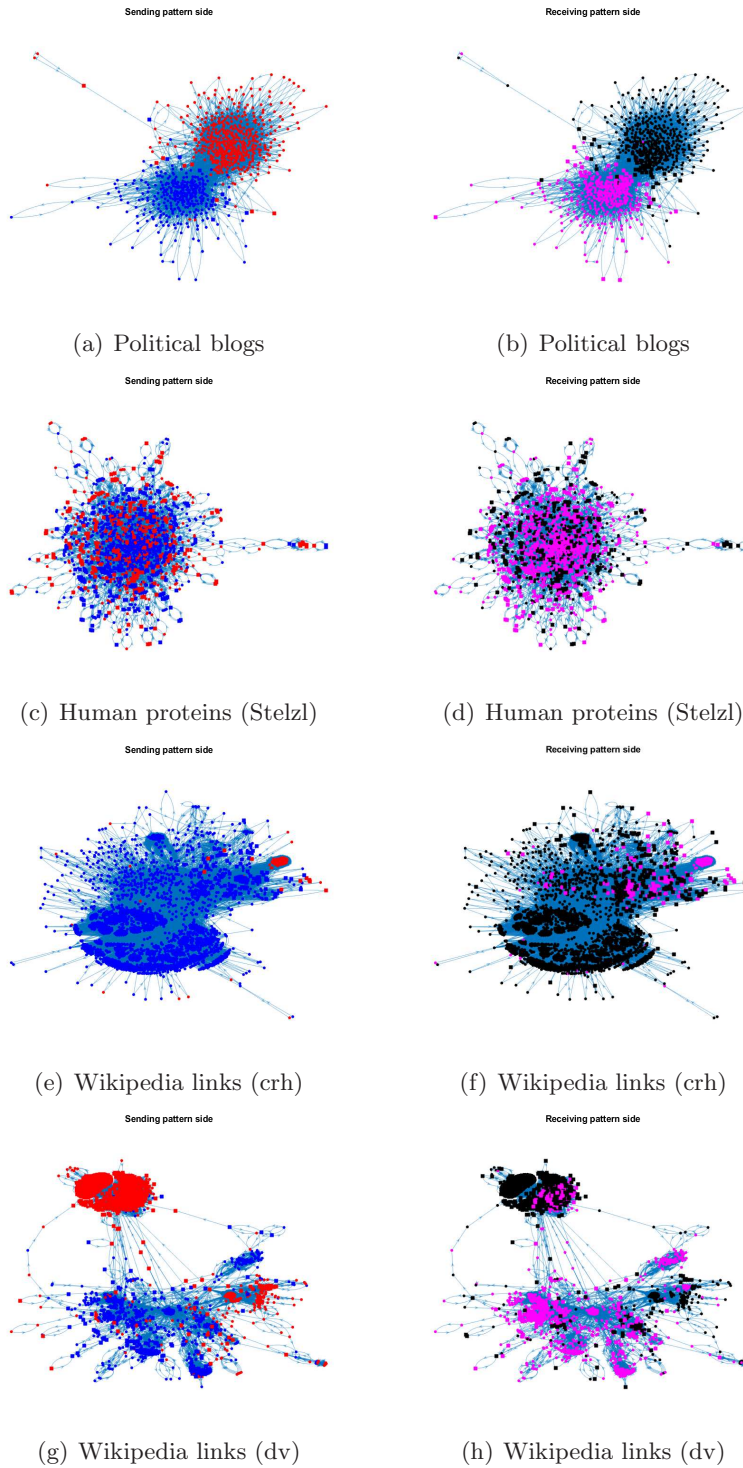


Figure 8: Sending and receiving clusters detected by DiSP for directed networks considered in this paper. Colors indicate clusters and square indicates highly mixed nodes, where sending and receiving clusters are obtained by  $\hat{\ell}_r$  and  $\hat{\ell}_c$ , respectively.

Table 1: The proportion of highly mixed nodes and the asymmetric structure measured by MHamm for real world directed networks used in this paper by applying DiSP to their adjacency matrices assuming that there are  $K = 2$  row (column) communities.

data	$\tau_r$	$\tau_c$	MHamm
Political blogs	0.0246	0.1353	0.0901
Human proteins (Stelzl)	0.2986	0.2999	0.0115
Wikipedia links (crh)	0.0444	0.1308	0.0643
Wikipedia links (dv)	0.4089	0.3008	0.1804

mixed membership network. When DiMMSB degenerates to MMSB, our theoretical results match that of Theorem 2.2 Jin et al. (2017) when their DCMM degenerates to MMSB under mild conditions. Through the applications on some real-world directed networks, DiSP finds the highly mixed nodes, and it also reveals new insights on the asymmetries in the structure of these directed networks. The model DiMMSB developed in this paper is useful to model directed networks and generate directed mixed membership networks with true background membership matrices. The proposed algorithm DiSP designed is useful in studying the asymmetric structure between sending and receiving clusters for a directed network. We expect that the model DiMMSB and the algorithm DiSP will have applications beyond this paper and can be widely applied to study the properties of directed networks in network science.

## Acknowledgements

The authors would like to thank Dr. Edoardo M. Airolidi and Dr. Xiaopei Wang for sharing codes of vEM Airolidi et al. (2013) with us.

## Appendix A. Proof for identifiability

### A.1 Proof of Proposition 1

**Proof** To proof the identifiability, we follow similar idea as the proof of (a) in Theorem 2.1 Mao et al. (2020) which provides the proof of identifiability of MMSB. Let  $\Omega = U\Lambda V'$  be the compact singular value decomposition of  $\Omega$ . By Lemma 1,  $U = \Pi_r B_r, V = \Pi_c B_c$ . Thus, for any node  $i$ ,  $U(i, :)$  lies in the convex hull of the  $K$  rows of  $B_r$ , i.e.,  $U(i, :) \subseteq \text{Conv}(B_r)$  for  $1 \leq i \leq n_r$ . Similarly, we have  $V(j, :) \subseteq \text{Conv}(B_c)$  for  $1 \leq j \leq n_c$ , where we use  $\text{Conv}(M)$  denote the convex hull of the rows of the matrix  $M$ .

Now, if  $\Omega$  can be generated by another set of parameters  $(\tilde{\Pi}_r, \tilde{P}, \tilde{\Pi}_c)$  (i.e.,  $\Omega = \Pi_r P \Pi_c' = \tilde{\Pi}_r \tilde{P} \tilde{\Pi}_c'$ ), where  $\tilde{\Pi}_r$  and  $\tilde{\Pi}_c$  have different pure nodes sets, with indices  $\tilde{\mathcal{I}}_r \neq 1 : K, \tilde{\mathcal{I}}_c \neq 1 : K$ . By the previous argument, we have  $U(\tilde{\mathcal{I}}_r, :) \subseteq \text{Conv}(B_r)$  and  $V(\tilde{\mathcal{I}}_c, :) \subseteq \text{Conv}(B_c)$ . Since  $(\Pi_r, P, \Pi_c)$  and  $(\tilde{\Pi}_r, \tilde{P}, \tilde{\Pi}_c)$  generate the same  $\Omega$ , they have the same compact singular value decomposition up to a permutation of communities. Thus, swapping the roles of  $\Pi_r$  and  $\tilde{\Pi}_r$ , and reapplying the above argument, we have  $B_r \subseteq \text{Conv}(U(\tilde{\mathcal{I}}_r, :))$ . Then  $\text{Conv}(B_r) \subseteq \text{Conv}(U(\tilde{\mathcal{I}}_r, :)) \subseteq \text{Conv}(B_r)$ , therefore we must have  $\text{Conv}(B_r) = \text{Conv}(U(\tilde{\mathcal{I}}_r, :))$ . This

means that pure nodes in  $\Pi_r$  and  $\tilde{\Pi}_r$  are aligned up to a permutation, i.e.,  $U(\tilde{\mathcal{I}}_r, :) = M_r B_r$ , where  $M_r \in \mathbb{R}^{K \times K}$  is a permutation matrix. Similarly, we have  $V(\tilde{\mathcal{I}}_c, :) = M_c B_c$ , where  $M_c \in \mathbb{R}^{K \times K}$  is a permutation matrix.

By Lemma 1, we have  $U = \Pi_r B_r$  and  $U = \tilde{\Pi}_r U(\tilde{\mathcal{I}}_r, :)$ , combining with  $U(\tilde{\mathcal{I}}_r, :) = M_r B_r$ , we have

$$(\Pi_r - \tilde{\Pi}_r M_r) B_r = 0.$$

Since  $\text{rank}(P) = K$  based on Condition (I1), we have  $\text{rank}(B_r) = K$ , i.e.,  $B_r$  is full rank. So we have  $\Pi_r = \tilde{\Pi}_r M_r$ . Thus,  $\Pi_r$  and  $\tilde{\Pi}_r$  are identical up to a permutation. Similarly,  $\Pi_c = \tilde{\Pi}_c M_c$ , i.e.,  $\Pi_c$  and  $\tilde{\Pi}_c$  are identical up to a permutation. To have the same  $\Omega$ , we have

$$\begin{aligned} \Pi_r P \Pi_c' &= \tilde{\Pi}_r \tilde{P} \tilde{\Pi}_c' \\ &\Downarrow \\ \tilde{\Pi}_r M_r P (\tilde{\Pi}_c M_c)' &= \tilde{\Pi}_r \tilde{P} \tilde{\Pi}_c' \\ &\Downarrow \\ M_r P M_c' &= \tilde{P}, \end{aligned}$$

where the last equality holds by Lemma 7 and condition (I2).  $M_r P M_c' = \tilde{P}$  gives that  $P$  and  $\tilde{P}$  are identical up to a row permutation and a column permutation.

**Lemma 7** *For any membership matrix  $\Pi \in \mathbb{R}^{n \times K}$  whose  $i$ -th row  $[\Pi(i, 1), \Pi(i, 2), \dots, \Pi(i, K)]$  is the PMF of node  $i$  for  $1 \leq i \leq n$ , such that each community has at least one pure node, then for any  $X, \tilde{X} \in \mathbb{R}^{K \times K}$ , if  $\Pi X = \Pi \tilde{X}$ , we have  $X = \tilde{X}$ .*

**Proof** Assume that node  $i$  is a pure node such that  $\Pi(i, k) = 1$ , then the  $i$ -th row of  $\Pi X$  is  $[X(k, 1), X(k, 2), \dots, X(k, K)]$  (i.e., the  $i$ -th row of  $\Pi X$  is the  $k$ -th row of  $X$  if  $\Pi(i, k) = 1$ ); similarly, the  $i$ -th row of  $\Pi \tilde{X}$  is the  $k$ -th row of  $\tilde{X}$ . Since  $\Pi X = \Pi \tilde{X}$ , we have  $[X(k, 1), X(k, 2), \dots, X(k, K)] = [\tilde{X}(k, 1), \tilde{X}(k, 2), \dots, \tilde{X}(k, K)]$  for  $1 \leq k \leq K$ , hence  $X = \tilde{X}$ . ■

**Remark 5** *Here, we propose an alternative proof of DiMMSB's identifiability. As in the main text, we always set  $\Pi_r(\mathcal{I}_r, :) = I_K$  and  $\Pi_c(\mathcal{I}_c, :) = I_K$ . By Lemma 1, we have  $U = \Pi_r U(\mathcal{I}_r, :) = \tilde{\Pi}_r U(\mathcal{I}_r, :)$  and  $U(\mathcal{I}_r, :)$  is invertible based on Conditions (I1) and (I2), which gives  $\Pi_r = \tilde{\Pi}_r$ . Similarly, we have  $\Pi_c = \tilde{\Pi}_c$ . By Lemma 7, we have  $P = \tilde{P}$ . here, there is no need to consider permutation since we set  $\Pi_r(\mathcal{I}_r, :) = I_K$  and  $\Pi_c(\mathcal{I}_c, :) = I_K$ . Note that, in this proof, the invertibility of  $U(\mathcal{I}_r, :)$  and  $V(\mathcal{I}_c, :)$  requires the number of row communities equals that of column communities, and this is the reason we do not model a directed mixed membership network whose number of row communities does not equal that of column communities in the definition of DiMMSB.* ■

## Appendix B. Ideal simplex

### B.1 Proof of Lemma 1

**Proof** Since  $\Omega = U\Lambda V'$  and  $V'V = I_K$ , we have  $U = \Omega V\Lambda^{-1}$ . Recall that  $\Omega = \Pi_r P \Pi_c'$ , we have  $U = \Pi_r P \Pi_c' V\Lambda^{-1} = \Pi_r B_r$ , where we set  $B_r = P \Pi_c' V\Lambda^{-1}$ . Since  $U(\mathcal{I}_r, :) = \Pi_r(\mathcal{I}_r, :) B_r = B_r$ , we have  $B_r = U(\mathcal{I}_r, :)$ . For  $1 \leq i \leq n_r$ ,  $U(i, :) = e_i' \Pi_r B_r = \Pi_r(i, :) B_r$ , so sure we have  $U(i, :) = U(\bar{i}, :)$  when  $\Pi_r(i, :) = \Pi_r(\bar{i}, :)$ . Follow similar analysis for  $V$ , and this lemma holds surely.  $\blacksquare$

### B.2 Proof of Theorem 1

**Proof** For column nodes, Remark 6 guarantees that SP algorithm returns  $\mathcal{I}_r$  when the input is  $U$  with  $K$  row communities, hence Ideal DiSP recovers  $\Pi_r$  exactly. Similar for recovering  $\Pi_c$  from  $V$ , and this theorem follows.  $\blacksquare$

### B.3 Proof of Lemma 2

**Proof** By Lemma 1, we know that  $U = \Pi_r U(\mathcal{I}_r, :)$ , which gives that  $U_2 = UU' = \Pi_r U(\mathcal{I}_r, :)' U' = \Pi_r(UU')(\mathcal{I}_r, :) = \Pi_r U_2(\mathcal{I}_r, :)$ . Similar for  $V_2$ , thus this lemma holds.  $\blacksquare$

## Appendix C. Basic properties of $\Omega$

**Lemma 8** Under DiMMSB( $n_r, n_c, K, P, \Pi_r, \Pi_c$ ), we have

$$\begin{aligned} \sqrt{\frac{1}{K\lambda_1(\Pi_r'\Pi_r)}} &\leq \|U(i, :)\|_F \leq \sqrt{\frac{1}{\lambda_K(\Pi_r'\Pi_r)}}, & 1 \leq i \leq n_r, \\ \sqrt{\frac{1}{K\lambda_1(\Pi_c'\Pi_c)}} &\leq \|V(j, :)\|_F \leq \sqrt{\frac{1}{\lambda_K(\Pi_c'\Pi_c)}}, & 1 \leq j \leq n_c. \end{aligned}$$

**Proof** For  $\|U(i, :)\|_F$ , since  $U = \Pi_r B_r$ , we have

$$\begin{aligned} \min_i \|e_i' U\|_F^2 &= \min_i e_i' U U' e_i = \min_i \Pi_r(i, :) B_r B_r' \Pi_r'(i, :) = \min_i \|\Pi_r(i, :)\|_F^2 \frac{\Pi_r(i, :)}{\|\Pi_r(i, :)\|_F} B_r B_r' \frac{\Pi_r'(i, :)}{\|\Pi_r(i, :)\|_F} \\ &\geq \min_i \|\Pi_r(i, :)\|_F^2 \min_{\|x\|_F=1} x' B_r B_r' x = \min_i \|\Pi_r(i, :)\|_F^2 \lambda_K(B_r B_r') \stackrel{\text{By Lemma 9}}{=} \frac{\min_i \|\Pi_r(i, :)\|_F^2}{\lambda_1(\Pi_r'\Pi_r)} \\ &\geq \frac{1}{K\lambda_1(\Pi_r'\Pi_r)}, \end{aligned}$$

where the last inequality holds because  $\|\Pi_r(i, :)\|_F \geq \|\Pi_r(i, :)\|_1 / \sqrt{K} = 1 / \sqrt{K}$  for  $1 \leq i \leq n_r$ . Meanwhile,

$$\max_i \|e_i' U\|_F^2 = \max_i \|\Pi_r(i, :)\|_F^2 \frac{\Pi_r(i, :)}{\|\Pi_r(i, :)\|_F} B_r B_r' \frac{\Pi_r'(i, :)}{\|\Pi_r(i, :)\|_F} \leq \max_i \|\Pi_r(i, :)\|_F^2 \max_{\|x\|_F=1} x' B_r B_r' x$$



$$= \max_i \|\Pi_r(i, :)\|_F^2 \lambda_1(B_r B_r') \stackrel{\text{By Lemma 9}}{=} \frac{\max_i \|\Pi_r(i, :)\|_F^2}{\lambda_K(\Pi_r' \Pi_r)} \leq \frac{1}{\lambda_K(\Pi_r' \Pi_r)}.$$

This lemma holds by following similar proof for  $\|V(j, :)\|_F$ . ■

**Lemma 9** *Under DiMMSB( $n_r, n_c, K, P, \Pi_r, \Pi_c$ ), we have*

$$\lambda_1(B_r B_r') = \frac{1}{\lambda_K(\Pi_r' \Pi_r)}, \lambda_K(B_r B_r') = \frac{1}{\lambda_1(\Pi_r' \Pi_r)}, \text{ and } \lambda_1(B_c B_c') = \frac{1}{\lambda_K(\Pi_c' \Pi_c)}, \lambda_K(B_c B_c') = \frac{1}{\lambda_1(\Pi_c' \Pi_c)}.$$

**Proof** Recall that  $U = \Pi_r B_r$  and  $U'U = I$ , we have  $I = B_r' \Pi_r' \Pi_r B_r$ . As  $B_r$  is full rank, we have  $\Pi_r' \Pi_r = (B_r B_r')^{-1}$ , which gives

$$\lambda_1(B_r B_r') = \frac{1}{\lambda_K(\Pi_r' \Pi_r)}, \lambda_K(B_r B_r') = \frac{1}{\lambda_1(\Pi_r' \Pi_r)}.$$

Follow similar proof for  $B_c B_c'$ , this lemma follows. ■

**Lemma 10** *Under DiMMSB( $n_r, n_c, K, P, \Pi_r, \Pi_c$ ), we have*

$$\sigma_K(\Omega) \geq \rho \sigma_K(\tilde{P}) \sigma_K(\Pi_r) \sigma_K(\Pi_c) \text{ and } \sigma_1(\Omega) \leq \rho \sigma_1(\tilde{P}) \sigma_1(\Pi_r) \sigma_1(\Pi_c).$$

**Proof** For  $\sigma_K(\Omega)$ , we have

$$\begin{aligned} \sigma_K^2(\Omega) &= \lambda_K(\Omega \Omega') = \lambda_K(\Pi_r P \Pi_c' \Pi_c P' \Pi_r') = \lambda_K(\Pi_r' \Pi_r P \Pi_c' \Pi_c P') \\ &\geq \lambda_K(\Pi_r' \Pi_r) \lambda_K(P \Pi_c' \Pi_c P') = \lambda_K(\Pi_r' \Pi_r) \lambda_K(\Pi_c' \Pi_c P' P) \\ &\geq \lambda_K(\Pi_r' \Pi_r) \lambda_K(\Pi_c' \Pi_c) \lambda_K(P P') = \rho^2 \sigma_K^2(\Pi_r) \sigma_K^2(\Pi_c) \sigma_K^2(\tilde{P}), \end{aligned}$$

where we have used the fact for any matrices  $X, Y$ , the nonzero eigenvalues of  $XY$  are the same as the nonzero eigenvalues of  $YX$ .

For  $\sigma_1(\Omega)$ , since  $\Omega = \Pi_r P \Pi_c' = \rho \Pi_r \tilde{P} \Pi_c'$ , we have

$$\sigma_1(\Omega) = \|\Omega\| = \rho \|\Pi_r \tilde{P} \Pi_c'\| \leq \rho \|\Pi_r\| \|\tilde{P}\| \|\Pi_c'\| = \rho \sigma_1(P) \sigma_1(\Pi_r) \sigma_1(\Pi_c).$$

■

## Appendix D. Proof of consistency of DiSP

### D.1 Proof of Lemma 3

**Proof** We use the rectangular version of Bernstein inequality in Tropp (2012) to bound  $\|A - \Omega\|$ . First, we write the rectangular version of Bernstein inequality as follows:

**Theorem 3** Consider a sequence  $\{X_k\}$  of  $d_1 \times d_1$  random matrices that satisfy the assumptions

$$\mathbb{E}(X_k) = 0 \quad \text{and} \quad \|X_k\| \leq R \quad \text{almost surely,}$$

then

$$\mathbb{P}(\|\sum_k X_k\| \geq t) \leq (d_1 + d_2) \cdot \exp\left(\frac{-t^2/2}{\sigma^2 + Rt/3}\right),$$

where the variance parameter

$$\sigma^2 := \max(\|\sum_k \mathbb{E}(X_k X_k')\|, \|\sum_k \mathbb{E}(X_k' X_k)\|).$$

Let  $e_i$  be an  $n_r \times 1$  vector, where  $e_i(i) = 1$  and 0 elsewhere, for row nodes  $1 \leq i \leq n_r$ , and  $\tilde{e}_j$  be an  $n_c \times 1$  vector, where  $\tilde{e}_j(j) = 1$  and 0 elsewhere, for column nodes  $1 \leq j \leq n_c$ . Then we can write  $W$  as  $W = \sum_{i=1}^{n_r} \sum_{j=1}^{n_c} W(i, j) e_i \tilde{e}_j'$ , where  $W = A - \Omega$ . Set  $W^{(i, j)}$  as the  $n_r \times n_c$  matrix such that  $W^{(i, j)} = W(i, j) e_i \tilde{e}_j'$ , for  $1 \leq i \leq n_r, 1 \leq j \leq n_c$ . Surely, we have  $\mathbb{E}(W^{(i, j)}) = 0$ . By the definition of the matrix spectral norm, for  $1 \leq i \leq n_r, 1 \leq j \leq n_c$ , we have

$$\|W^{(i, j)}\| = \|W(i, j) e_i \tilde{e}_j'\| = |W(i, j)| \|e_i \tilde{e}_j'\| = |W(i, j)| = |A(i, j) - \Omega(i, j)| \leq 1.$$

Next we consider the variance parameter

$$\sigma^2 := \max(\|\sum_{i=1}^{n_r} \sum_{j=1}^{n_c} \mathbb{E}(W^{(i, j)} (W^{(i, j)})')\|, \|\sum_{i=1}^{n_r} \sum_{j=1}^{n_c} \mathbb{E}((W^{(i, j)})' W^{(i, j)})\|).$$

Since  $\Omega(i, j) = \mathbb{E}(A(i, j))$ , we can obtain the bound of  $\mathbb{E}(W^2(i, j))$  first. We have

$$\mathbb{E}(W^2(i, j)) = \mathbb{E}((A(i, j) - \Omega(i, j))^2) = \mathbb{E}((A(i, j) - \mathbb{E}(A(i, j)))^2) = \text{Var}(A(i, j)),$$

where  $\text{Var}(A(i, j))$  denotes the variance of Bernoulli random variable  $A(i, j)$ . Then we have

$$\mathbb{E}(W^2(i, j)) = \text{Var}(A(i, j)) = \mathbb{P}(A(i, j) = 1)(1 - \mathbb{P}(A(i, j) = 1)) \leq \mathbb{P}(A(i, j) = 1) = \Omega(i, j) = e_i' \Pi_r \rho \tilde{P} \Pi_c' \tilde{e}_j \leq \rho.$$

Since  $e_i e_i'$  is an  $n_r \times n_r$  diagonal matrix with  $(i, i)$ -th entry being 1 and others entries being 0, then we bound  $\|\sum_{i=1}^{n_r} \sum_{j=1}^{n_c} \mathbb{E}(W^{(i, j)} (W^{(i, j)})')\|$  as

$$\begin{aligned} \|\sum_{i=1}^{n_r} \sum_{j=1}^{n_c} \mathbb{E}(W^{(i, j)} (W^{(i, j)})')\| &= \|\sum_{i=1}^{n_r} \sum_{j=1}^{n_c} \mathbb{E}(W^2(i, j)) e_i \tilde{e}_j' \tilde{e}_j e_i'\| = \|\sum_{i=1}^{n_r} \sum_{j=1}^{n_c} \mathbb{E}(W^2(i, j)) e_i e_i'\| \\ &= \max_{1 \leq i \leq n_r} \left| \sum_{j=1}^{n_c} \mathbb{E}(W^2(i, j)) \right| \leq \rho n_c. \end{aligned}$$

Similarly, we have  $\|\sum_{i=1}^{n_r} \sum_{j=1}^{n_c} \mathbb{E}((W^{(i, j)})' W^{(i, j)})\| \leq \rho n_r$ . Thus, we have

$$\sigma^2 = \max(\|\sum_{i=1}^{n_r} \sum_{j=1}^{n_c} \mathbb{E}(W^{(i, j)} (W^{(i, j)})')\|, \|\sum_{i=1}^{n_r} \sum_{j=1}^{n_c} \mathbb{E}((W^{(i, j)})' W^{(i, j)})\|) \leq \rho \max(n_r, n_c).$$

By the rectangular version of Bernstein inequality, combining with  $\sigma^2 \leq \rho \max(n_r, n_c)$ ,  $R = 1$ ,  $d_1 + d_2 = n_r + n_c$ , set  $t = \frac{\alpha+1+\sqrt{\alpha^2+20\alpha+19}}{3} \sqrt{\rho \max(n_r, n_c) \log(n_r + n_c)}$ , we have

$$\begin{aligned} \mathbb{P}(\|W\| \geq t) &= \mathbb{P}\left(\left\|\sum_{i=1}^{n_r} \sum_{j=1}^{n_c} W^{(i,j)}\right\| \geq t\right) = (n_r + n_c) \exp\left(-\frac{t^2/2}{\sigma^2 + \frac{Rt}{3}}\right) \leq (n_r + n_c) \exp\left(-\frac{t^2/2}{\rho \max(n_r, n_c) + t/3}\right) \\ &= (n_r + n_c) \exp(-(\alpha + 1) \log(n_r + n_c)) \cdot \frac{1}{\frac{2(\alpha+1)\rho \max(n_r, n_c) \log(n_r + n_c)}{t^2} + \frac{2(\alpha+1) \log(n_r + n_c)}{3t}} \\ &= (n_r + n_c) \exp(-(\alpha + 1) \log(n_r + n_c)) \cdot \frac{1}{\frac{18}{(\sqrt{\alpha+19} + \sqrt{\alpha+1})^2} + \frac{2\sqrt{\alpha+1}}{\sqrt{\alpha+19} + \sqrt{\alpha+1}} \sqrt{\frac{\log(n_r + n_c)}{\rho \max(n_r, n_c)}}} \\ &\leq (n_r + n_c) \exp(-(\alpha + 1) \log(n_r + n_c)) = \frac{1}{(n_r + n_c)^\alpha}, \end{aligned}$$

where we have used the assumption (1) and the fact that  $\frac{18}{(\sqrt{\alpha+19} + \sqrt{\alpha+1})^2} + \frac{2\sqrt{\alpha+1}}{\sqrt{\alpha+19} + \sqrt{\alpha+1}} \sqrt{\frac{\log(n_r + n_c)}{\rho \max(n_r, n_c)}} \leq \frac{18}{(\sqrt{\alpha+19} + \sqrt{\alpha+1})^2} + \frac{2\sqrt{\alpha+1}}{\sqrt{\alpha+19} + \sqrt{\alpha+1}} = 1$  in the last inequality. Thus, the claim follows.  $\blacksquare$

## D.2 Proof of Lemma 4

**Proof** We use Theorem 4.3.1 Chen et al. (2020) to bound  $\|\hat{U} \text{sgn}(H_{\hat{U}}) - U\|_{2 \rightarrow \infty}$  and  $\|\hat{V} \text{sgn}(H_{\hat{V}}) - V\|_{2 \rightarrow \infty}$  where  $\text{sgn}(H_{\hat{U}})$  and  $\text{sgn}(H_{\hat{V}})$  are defined later. Let  $H_{\hat{U}} = \hat{U}' U$ , and  $H_{\hat{U}} = U_{H_{\hat{U}}} \Sigma_{H_{\hat{U}}} V_{H_{\hat{U}}}'$  be the SVD decomposition of  $H_{\hat{U}}$  with  $U_{H_{\hat{U}}}, V_{H_{\hat{U}}} \in \mathbb{R}^{n_r \times K}$ , where  $U_{H_{\hat{U}}}$  and  $V_{H_{\hat{U}}}$  represent respectively the left and right singular matrices of  $H_{\hat{U}}$ . Define  $\text{sgn}(H_{\hat{U}}) = U_{H_{\hat{U}}} V_{H_{\hat{U}}}'$ .  $\text{sgn}(H_{\hat{V}})$  is defined similarly. Since  $\mathbb{E}(A(i, j) - \Omega(i, j)) = 0$ ,  $\mathbb{E}[(A(i, j) - \Omega(i, j))^2] \leq \rho$  by the proof of Lemma 3,  $\frac{1}{\sqrt{\rho \min(n_r, n_c) / (\mu \log(n_r + n_c))}} \leq O(1)$  holds by assumption (1). Then by Theorem 4.3.1. Chen et al. (2020), with high probability,

$$\max(\|\hat{U} \text{sgn}(H_{\hat{U}}) - U\|_{2 \rightarrow \infty}, \|\hat{V} \text{sgn}(H_{\hat{V}}) - V\|_{2 \rightarrow \infty}) \leq C \frac{\sqrt{\rho K} (\kappa(\Omega) \sqrt{\frac{\max(n_r, n_c) \mu}{\min(n_r, n_c)}} + \sqrt{\log(n_r + n_c)})}{\sigma_K(\Omega)},$$

provided that  $c_1 \sigma_K(\Omega) \geq \sqrt{\rho(n_r + n_c) \log(n_r + n_c)}$  for some sufficiently small constant  $c_1$ .

Now we are ready to bound  $\|\hat{U} \hat{U}' - U U'\|_{2 \rightarrow \infty}$  and  $\|\hat{V} \hat{V}' - V V'\|_{2 \rightarrow \infty}$ . Since  $\hat{U}' \hat{U} = I$ , by basic algebra, we have

$$\begin{aligned} \|\hat{U} \hat{U}' - U U'\|_{2 \rightarrow \infty} &\leq 2\|U - \hat{U} \text{sgn}(H_{\hat{U}})\|_{2 \rightarrow \infty} \leq C \frac{\sqrt{K} \sqrt{\rho} (\kappa(\Omega) \sqrt{\frac{\max(n_r, n_c) \mu}{\min(n_r, n_c)}} + \sqrt{\log(n_r + n_c)})}{\sigma_K(\Omega)} \\ &\stackrel{\text{By Lemma 10}}{\leq} C \frac{\sqrt{K} (\kappa(\Omega) \sqrt{\frac{\max(n_r, n_c) \mu}{\min(n_r, n_c)}} + \sqrt{\log(n_r + n_c)})}{\sigma_K(\hat{P}) \sigma_K(\Pi_r) \sigma_K(\Pi_c) \sqrt{\rho}}. \end{aligned}$$

The lemma holds by following similar proof for  $\|\hat{V} \hat{V}' - V V'\|_{2 \rightarrow \infty}$ .  $\blacksquare$

### D.3 Proof of Lemma 5

**Proof** First, we write down the SP algorithm as below. Based on Algorithm 4, the following

---

**Algorithm 4 Successive Projection (SP)** Gillis and Vavasis (2015)

---

**Require:** Near-separable matrix  $Y_{sp} = S_{sp}M_{sp} + Z_{sp} \in \mathbb{R}_+^{m \times n}$ , where  $S_{sp}, M_{sp}$  should satisfy Assumption 1 Gillis and Vavasis (2015), the number  $r$  of columns to be extracted.

**Ensure:** Set of indices  $\mathcal{K}$  such that  $Y_{sp}(\mathcal{K}, :) \approx S$  (up to permutation)

- 1: Let  $R = Y_{sp}, \mathcal{K} = \{1\}, k = 1$ .
  - 2: **While**  $R \neq 0$  and  $k \leq r$  **do**
  - 3:      $k_* = \operatorname{argmax}_k \|R(k, :)\|_F$ .
  - 4:      $u_k = R(k_*, :)$ .
  - 5:      $R \leftarrow (I - \frac{u_k u_k'}{\|u_k\|_F^2})R$ .
  - 6:      $\mathcal{K} = \mathcal{K} \cup \{k_*\}$ .
  - 7:      $k = k + 1$ .
  - 8: **end while**
- 

theorem is Theorem 1.1 in Gillis and Vavasis (2015).

**Theorem 4** Fix  $m \geq r$  and  $n \geq r$ . Consider a matrix  $Y_{sp} = S_{sp}M_{sp} + Z_{sp}$ , where  $S_{sp} \in \mathbb{R}^{m \times r}$  has a full column rank,  $M_{sp} \in \mathbb{R}^{r \times n}$  is a nonnegative matrix such that the sum of each column is at most 1, and  $Z_{sp} = [Z_{sp,1}, \dots, Z_{sp,n}] \in \mathbb{R}^{m \times n}$ . Suppose  $M_{sp}$  has a submatrix equal to  $I_r$ . Write  $\epsilon \leq \max_{1 \leq i \leq n} \|Z_{sp,i}\|_F$ . Suppose  $\epsilon = O(\frac{\sigma_{\min}(S_{sp})}{\sqrt{r\kappa^2(S_{sp})}})$ , where  $\sigma_{\min}(S_{sp})$  and  $\kappa(S_{sp})$  are the minimum singular value and condition number of  $S_{sp}$ , respectively. If we apply the SP algorithm to columns of  $Y_{sp}$ , then it outputs an index set  $\mathcal{K} \subset \{1, 2, \dots, n\}$  such that  $|\mathcal{K}| = r$  and  $\max_{1 \leq k \leq r} \min_{j \in \mathcal{K}} \|S_{sp}(:, k) - Y_{sp}(:, j)\|_F = O(\epsilon \kappa^2(S_{sp}))$ , where  $S_{sp}(:, k)$  is the  $k$ -th column of  $S_{sp}$ .

First, we consider row nodes. Let  $m = K, r = K, n = n_r, Y_{sp} = \hat{U}_2', Z = \hat{U}_2' - U_2', S_{sp} = U_2'(\mathcal{I}_r, :)$ , and  $M_{sp} = \Pi_r'$ . By condition (I2),  $M_{sp}$  has an identity submatrix  $I_K$ . By Lemma 4, we have

$$\epsilon = \max_{1 \leq i \leq n_r} \|\hat{U}_2'(i, :) - U_2'(i, :)\|_F = \|\hat{U}_2'(i, :) - U_2'(i, :)\|_{2 \rightarrow \infty} \leq \varpi.$$

By Theorem 4, there exists a permutation matrix  $\mathcal{P}_r$  such that

$$\max_{1 \leq k \leq K} \|e_k'(\hat{U}_2'(\hat{\mathcal{I}}_r, :) - \mathcal{P}_r' U_2'(\mathcal{I}_r, :))\|_F = O(\epsilon \kappa^2(U_2'(\mathcal{I}_r, :)) \sqrt{K}) = O(\varpi \kappa^2(U_2'(\mathcal{I}_r, :))).$$

Since  $\kappa^2(U_2'(\mathcal{I}_r, :)) = \kappa(U_2'(\mathcal{I}_r, :) U_2'(\mathcal{I}_r, :)) = \kappa(U(\mathcal{I}_r, :) U'(\mathcal{I}_r, :)) = \kappa(\Pi_r' \Pi_r)$  where the last equality holds by Lemma 9, we have

$$\max_{1 \leq k \leq K} \|e_k'(\hat{U}_2'(\hat{\mathcal{I}}_r, :) - \mathcal{P}_r' U_2'(\mathcal{I}_r, :))\|_F = O(\varpi \kappa(\Pi_r' \Pi_r)).$$

Follow similar analysis for column nodes, we have

$$\max_{1 \leq k \leq K} \|e_k'(\hat{V}_2(\hat{\mathcal{I}}_c, :) - \mathcal{P}_c' V_2(\mathcal{I}_c, :))\|_F = O(\varpi \kappa(\Pi_c' \Pi_c)).$$

**Remark 6** For the ideal case, let  $m = K, r = K, n = n_c, Y_{sp} = U', Z_{sp} = U' - U' \equiv 0, S_{sp} = U'(\mathcal{I}_r, :)$ , and  $M_{sp} = \Pi'_r$ . Then, we have  $\max_{1 \leq i \leq n_r} \|U(i, :) - U(i, :)\|_F = 0$ . By Theorem 4, SP algorithm returns  $\mathcal{I}_r$  when the input is  $U$  assuming there are  $K$  row communities. ■

#### D.4 Proof of Lemma 6

**Proof** First, we consider row nodes. Recall that  $U(\mathcal{I}_r, :) = B_r$ . For convenience, set  $\hat{U}(\hat{\mathcal{I}}_r, :) = \hat{B}_r, U_2(\mathcal{I}_r, :) = B_{2r}, \hat{U}_2(\hat{\mathcal{I}}_r, :) = \hat{B}_{2r}$ . We bound  $\|e'_i(\hat{Y}_r - Y_r \mathcal{P}_r)\|_F$  when the input is  $\hat{U}$  in the SP algorithm. Recall that  $Y_r = \max(UU'(\mathcal{I}_r, :)(U(\mathcal{I}_r, :)U'(\mathcal{I}_r, :))^{-1}, 0) \equiv \Pi_r$ , for  $1 \leq i \leq n_r$ , we have

$$\begin{aligned}
 \|e'_i(\hat{Y}_r - Y_r \mathcal{P}_r)\|_F &= \|e'_i(\max(0, \hat{U} \hat{B}'_r (\hat{B}_r \hat{B}'_r)^{-1}) - U B'_r (B_r B'_r)^{-1} \mathcal{P}_r)\|_F \\
 &\leq \|e'_i(\hat{U} \hat{B}'_r (\hat{B}_r \hat{B}'_r)^{-1} - U B'_r (B_r B'_r)^{-1} \mathcal{P}_r)\|_F \\
 &= \|e'_i(\hat{U} - U(U' \hat{U})) \hat{B}'_r (\hat{B}_r \hat{B}'_r)^{-1} + e'_i(U(U' \hat{U}) \hat{B}'_r (\hat{B}_r \hat{B}'_r)^{-1} - U(U' \hat{U})(\mathcal{P}'_r (B_r B'_r) (B'_r)^{-1} (U' \hat{U}))^{-1})\|_F \\
 &\leq \|e'_i(\hat{U} - U(U' \hat{U})) \hat{B}'_r (\hat{B}_r \hat{B}'_r)^{-1}\|_F + \|e'_i U(U' \hat{U})(\hat{B}'_r (\hat{B}_r \hat{B}'_r)^{-1} - (\mathcal{P}'_r (B_r B'_r) (B'_r)^{-1} (U' \hat{U}))^{-1})\|_F \\
 &\leq \|e'_i(\hat{U} - U(U' \hat{U}))\|_F \|\hat{B}_r^{-1}\|_F + \|e'_i U(U' \hat{U})(\hat{B}'_r (\hat{B}_r \hat{B}'_r)^{-1} - (\mathcal{P}'_r (B_r B'_r) (B'_r)^{-1} (U' \hat{U}))^{-1})\|_F \\
 &\leq \sqrt{K} \|e'_i(\hat{U} - U(U' \hat{U}))\|_F / \sqrt{\lambda_K(\hat{B}_r \hat{B}'_r)} + \|e'_i U(U' \hat{U})(\hat{B}_r^{-1} - (\mathcal{P}'_r B_r (U' \hat{U}))^{-1})\|_F \\
 &= \sqrt{K} \|e'_i(\hat{U} \hat{U}' - U U') \hat{U}\|_F O(\sqrt{\lambda_1(\Pi'_r \Pi_r)}) + \|e'_i U(U' \hat{U})(\hat{B}_r^{-1} - (\mathcal{P}'_r B_r (U' \hat{U}))^{-1})\|_F \\
 &\leq \sqrt{K} \|e'_i(\hat{U} \hat{U}' - U U')\|_F O(\sqrt{\lambda_1(\Pi'_r \Pi_r)}) + \|e'_i U(U' \hat{U})(\hat{B}_r^{-1} - (\mathcal{P}'_r B_r (U' \hat{U}))^{-1})\|_F \\
 &\leq \sqrt{K} \varpi O(\sqrt{\lambda_1(\Pi'_r \Pi_r)}) + \|e'_i U(U' \hat{U})(\hat{B}_r^{-1} - (\mathcal{P}'_r B_r (U' \hat{U}))^{-1})\|_F \\
 &= O(\varpi \sqrt{K \lambda_1(\Pi'_r \Pi_r)}) + \|e'_i U(U' \hat{U})(\hat{B}_r^{-1} - (\mathcal{P}'_r B_r (U' \hat{U}))^{-1})\|_F,
 \end{aligned}$$

where we have used similar idea in the proof of Lemma VII.3 in Mao et al. (2020) such that apply  $O(\frac{1}{\lambda_K(\hat{B}_r \hat{B}'_r)})$  to estimate  $\frac{1}{\lambda_K(\hat{B}_r \hat{B}'_r)}$ , then by Lemma 9, we have  $\frac{1}{\lambda_K(\hat{B}_r \hat{B}'_r)} = O(\lambda_1(\Pi'_r \Pi_r))$ .

Now we aim to bound  $\|e'_i U(U' \hat{U})(\hat{B}_r^{-1} - (\mathcal{P}'_r B_r (U' \hat{U}))^{-1})\|_F$ . For convenience, set  $T = U' \hat{U}, S = \mathcal{P}'_r B_r T$ . We have

$$\begin{aligned}
 \|e'_i U(U' \hat{U})(\hat{B}_r^{-1} - (\mathcal{P}'_r B_r (U' \hat{U}))^{-1})\|_F &= \|e'_i U T S^{-1} (S - \hat{B}_r) \hat{B}_r^{-1}\|_F \\
 &\leq \|e'_i U T S^{-1} (S - \hat{B}_r)\|_F \|\hat{B}_r^{-1}\|_F \leq \|e'_i U T S^{-1} (S - \hat{B}_r)\|_F \frac{\sqrt{K}}{|\lambda_K(\hat{B}_r)|} \\
 &= \|e'_i U T S^{-1} (S - \hat{B}_r)\|_F \frac{\sqrt{K}}{\sqrt{\lambda_K(\hat{B}_r \hat{B}'_r)}} \leq \|e'_i U T S^{-1} (S - \hat{B}_r)\|_F O(\sqrt{K \lambda_1(\Pi'_r \Pi_r)}) \\
 &= \|e'_i U T T^{-1} B'_r (B_r B'_r)^{-1} \mathcal{P}_r (S - \hat{B}_r)\|_F O(\sqrt{K \lambda_1(\Pi'_r \Pi_r)}) \\
 &= \|e'_i U B'_r (B_r B'_r)^{-1} \mathcal{P}_r (S - \hat{B}_r)\|_F O(\sqrt{K \lambda_1(\Pi'_r \Pi_r)}) \\
 &= \|e'_i Y_r \mathcal{P}_r (S - \hat{B}_r)\|_F O(\sqrt{K \lambda_1(\Pi'_r \Pi_r)}) \stackrel{\text{By } Y_r = \Pi_r}{\leq} \max_{1 \leq k \leq K} \|e'_k (S - \hat{B}_r)\|_F O(\sqrt{K \lambda_1(\Pi'_r \Pi_r)})
 \end{aligned}$$

$$\begin{aligned}
 &= \max_{1 \leq k \leq K} \|e'_k(\hat{B}_r - \mathcal{P}'_r B_r U' \hat{U})\|_F O(\sqrt{K \lambda_1(\Pi'_r \Pi_r)}) \\
 &= \max_{1 \leq k \leq K} \|e'_k(\hat{B}_r \hat{U}' - \mathcal{P}'_r B_r U') \hat{U}\|_F O(\sqrt{K \lambda_1(\Pi'_r \Pi_r)}) \\
 &\leq \max_{1 \leq k \leq K} \|e'_k(\hat{B}_r \hat{U}' - \mathcal{P}'_r B_r U')\|_F O(\sqrt{K \lambda_1(\Pi'_r \Pi_r)}) \\
 &= \max_{1 \leq k \leq K} \|e'_k(\hat{B}_{2r} - \mathcal{P}'_r B_{2r})\|_F O(\sqrt{K \lambda_1(\Pi'_r \Pi_r)}) \\
 &= O(\varpi \kappa(\Pi'_r \Pi_r) \sqrt{K \lambda_1(\Pi'_r \Pi_r)}). \tag{9}
 \end{aligned}$$

**Remark 7** Eq (9) supports our statement that building the theoretical framework of DiSP benefits a lot by introducing DiSP-equivalence algorithm since  $\|\hat{B}_{2r} - \mathcal{P}'_r B_{2r}\|_{2 \rightarrow \infty}$  is obtained from DiSP-equivalence (i.e., inputting  $\hat{U}_2$  in the SP algorithm obtains  $\|\hat{B}_{2r} - \mathcal{P}'_r B_{2r}\|_{2 \rightarrow \infty}$ . Similar benefits hold for column nodes.).

Then, we have

$$\begin{aligned}
 \|e'_i(\hat{Y}_r - Y_r \mathcal{P}_r)\|_F &\leq O(\varpi \sqrt{K \lambda_1(\Pi'_r \Pi_r)}) + \|e'_i U(U' \hat{U})(\hat{B}_r^{-1} - (\mathcal{P}'_r B_r (U' \hat{U}))^{-1})\|_F \\
 &\leq O(\varpi \sqrt{K \lambda_1(\Pi'_r \Pi_r)}) + O(\varpi \kappa(\Pi'_r \Pi_r) \sqrt{K \lambda_1(\Pi'_r \Pi_r)}) \\
 &= O(\varpi \kappa(\Pi'_r \Pi_r) \sqrt{K \lambda_1(\Pi'_r \Pi_r)}).
 \end{aligned}$$

Follow similar proof for column nodes, we have, for  $1 \leq j \leq n_c$ ,

$$\|e'_j(\hat{Y}_c - Y_c \mathcal{P}_c)\|_F = O(\varpi \kappa(\Pi'_c \Pi_c) \sqrt{K \lambda_1(\Pi'_c \Pi_c)}).$$

■

## D.5 Proof of Theorem 2

**Proof** Since

$$\begin{aligned}
 \|e'_i(\hat{\Pi}_r - \Pi_r \mathcal{P}_r)\|_1 &= \left\| \frac{e'_i \hat{Y}_r}{\|e'_i \hat{Y}_r\|_1} - \frac{e'_i Y_r \mathcal{P}_r}{\|e'_i Y_r \mathcal{P}_r\|_1} \right\|_1 = \left\| \frac{e'_i \hat{Y}_r \|e'_i Y_r\|_1 - e'_i Y_r \mathcal{P}_r \|e'_i \hat{Y}_r\|_1}{\|e'_i \hat{Y}_r\|_1 \|e'_i Y_r\|_1} \right\|_1 \\
 &= \left\| \frac{e'_i \hat{Y}_r \|e'_i Y_r\|_1 - e'_i \hat{Y}_r \|e'_i \hat{Y}_r\|_1 + e'_i \hat{Y}_r \|e'_i \hat{Y}_r\|_1 - e'_i Y_r \mathcal{P}_r \|e'_i \hat{Y}_r\|_1}{\|e'_i \hat{Y}_r\|_1 \|e'_i Y_r\|_1} \right\|_1 \\
 &\leq \frac{\|e'_i \hat{Y}_r \|e'_i Y_r\|_1 - e'_i \hat{Y}_r \|e'_i \hat{Y}_r\|_1\|_1 + \|e'_i \hat{Y}_r \|e'_i \hat{Y}_r\|_1 - e'_i Y_r \mathcal{P}_r \|e'_i \hat{Y}_r\|_1\|_1}{\|e'_i \hat{Y}_r\|_1 \|e'_i Y_r\|_1} \\
 &= \frac{\|e'_i \hat{Y}_r\|_1 \|e'_i Y_r\|_1 - \|e'_i \hat{Y}_r\|_1 + \|e'_i \hat{Y}_r\|_1 \|e'_i \hat{Y}_r - e'_i Y_r \mathcal{P}_r\|_1}{\|e'_i \hat{Y}_r\|_1 \|e'_i Y_r\|_1} \\
 &= \frac{\|e'_i Y_r\|_1 - \|e'_i \hat{Y}_r\|_1 + \|e'_i \hat{Y}_r - e'_i Y_r \mathcal{P}_r\|_1}{\|e'_i Y_r\|_1} \leq \frac{2\|e'_i(\hat{Y}_r - Y_r \mathcal{P}_r)\|_1}{\|e'_i Y_r\|_1} \\
 &= \frac{2\|e'_i(\hat{Y}_r - Y_r \mathcal{P}_r)\|_1}{\|e'_i \Pi_r\|_1} = 2\|e'_i(\hat{Y}_r - Y_r \mathcal{P}_r)\|_1 \leq 2\sqrt{K} \|e'_i(\hat{Y}_r - Y_r \mathcal{P}_r)\|_F,
 \end{aligned}$$

we have

$$\|e'_i(\hat{\Pi}_r - \Pi_r \mathcal{P}_r)\|_1 = O(\varpi \kappa(\Pi'_r \Pi_r) K \sqrt{\lambda_1(\Pi'_r \Pi_r)}).$$

Follow similar proof for column nodes, we have, for  $1 \leq j \leq n_c$ ,

$$\|e'_j(\hat{\Pi}_c - \Pi_c \mathcal{P}_c)\|_1 = O(\varpi \kappa(\Pi'_c \Pi_c) K \sqrt{\lambda_1(\Pi'_c \Pi_c)}).$$

■

## D.6 Proof of Corollary 1

**Proof** Under conditions of Corollary 1, we have

$$\begin{aligned} \|e'_i(\hat{\Pi}_r - \Pi_r \mathcal{P}_r)\|_1 &= O(\varpi K \sqrt{\frac{n_r}{K}}) = O(\varpi \sqrt{K n_r}), \\ \|e'_j(\hat{\Pi}_c - \Pi_c \mathcal{P}_c)\|_1 &= O(\varpi K \sqrt{\frac{n_c}{K}}) = O(\varpi \sqrt{K n_c}). \end{aligned}$$

Under conditions of Corollary 1,  $\kappa(\Omega) = O(1)$  by Lemma 10 and  $\mu = O(1) = C$  by Lemma 8 for some constant  $C > 0$ . Then, by Lemma 4, we have

$$\begin{aligned} \varpi &= O\left(\frac{\sqrt{K}(\kappa(\Omega) \sqrt{\frac{\max(n_r, n_c)\mu}{\min(n_r, n_c)}} + \sqrt{\log(n_r + n_c)})}{\sqrt{\rho} \sigma_K(\tilde{P}) \sigma_K(\Pi_r) \sigma_K(\Pi_c)}\right) = O\left(\frac{\sqrt{K}(\sqrt{C \frac{\max(n_r, n_c)}{\min(n_r, n_c)}} + \sqrt{\log(n_r + n_c)})}{\sqrt{\rho} \sigma_K(\tilde{P}) \sigma_K(\Pi_r) \sigma_K(\Pi_c)}\right) \\ &= O\left(\frac{\sqrt{K}(\sqrt{C \frac{\max(n_r, n_c)}{\min(n_r, n_c)}} + \sqrt{\log(n_r + n_c)})}{\sqrt{\rho} \sigma_K(\tilde{P}) \sqrt{n_r n_c} / K}\right) = O\left(\frac{K^{1.5}(\sqrt{C \frac{\max(n_r, n_c)}{\min(n_r, n_c)}} + \sqrt{\log(n_r + n_c)})}{\sigma_K(\tilde{P}) \sqrt{\rho n_r n_c}}\right), \end{aligned}$$

which gives that

$$\begin{aligned} \|e'_i(\hat{\Pi}_r - \Pi_r \mathcal{P}_r)\|_1 &= O\left(\frac{K^2(\sqrt{C \frac{\max(n_r, n_c)}{\min(n_r, n_c)}} + \sqrt{\log(n_r + n_c)})}{\sigma_K(\tilde{P}) \sqrt{\rho n_c}}\right), \\ \|e'_j(\hat{\Pi}_c - \Pi_c \mathcal{P}_c)\|_1 &= O\left(\frac{K^2(\sqrt{C \frac{\max(n_r, n_c)}{\min(n_r, n_c)}} + \sqrt{\log(n_r + n_c)})}{\sigma_K(\tilde{P}) \sqrt{\rho n_r}}\right). \end{aligned}$$

■

## References

- Emmanuel Abbe. Community detection and stochastic block models: recent developments. *The Journal of Machine Learning Research*, 18(1):6446–6531, 2017.
- Lada A. Adamic and Natalie Glance. The political blogosphere and the 2004 u.s. election: divided they blog. In *Proceedings of the 3rd international workshop on Link discovery*, pages 36–43, 2005.



- Edoardo M. Airoldi, David M. Blei, Stephen E. Fienberg, and Eric P. Xing. Mixed membership stochastic blockmodels. *Journal of Machine Learning Research*, 9:1981–2014, 2008.
- Edoardo M. Airoldi, Xiaopei Wang, and Xiaodong Lin. Multi-way blockmodels for analyzing coordinated high-dimensional responses. *The Annals of Applied Statistics*, 7(4):2431–2457, 2013.
- Punam Bedi and Chhavi Sharma. Community detection in social networks. *Wiley Interdisciplinary Reviews: Data Mining and Knowledge Discovery*, 6(3):115–135, 2016.
- Yudong Chen, Xiaodong Li, and Jiaming Xu. Convexified modularity maximization for degree-corrected stochastic block models. *Annals of Statistics*, 46(4):1573–1602, 2018.
- Yuxin Chen, Yuejie Chi, Jianqing Fan, and Cong Ma. Spectral methods for data science: A statistical perspective. *arXiv preprint arXiv:2012.08496*, 2020.
- Jennifer A. Dunne, Richard J. Williams, and Neo D. Martinez. Food-web structure and network theory: The role of connectance and size. *Proceedings of the National Academy of Sciences of the United States of America*, 99(20):12917, 2002.
- Jing Gao, Feng Liang, Wei Fan, Chi Wang, Yizhou Sun, and Jiawei Han. On community outliers and their efficient detection in information networks. In *Proceedings of the 16th ACM SIGKDD International Conference on Knowledge Discovery and Data Mining*, pages 813–822, 2010.
- Nicolas Gillis and Stephen A. Vavasis. Semidefinite programming based preconditioning for more robust near-separable nonnegative matrix factorization. *SIAM Journal on Optimization*, 25(1):677–698, 2015.
- Anna Goldenberg, Alice X. Zheng, Stephen E. Fienberg, and Edoardo M. Airoldi. A survey of statistical network models. *Foundations and Trends® in Machine Learning archive*, 2(2):129–233, 2010.
- P.K. Gopalan and D.M. Blei. Efficient discovery of overlapping communities in massive networks. *Proceedings of the National Academy of Sciences of the United States of America*, 110(36):14534–14539, 2013.
- Paul W. Holland, Kathryn Blackmond Laskey, and Samuel Leinhardt. Stochastic blockmodels: First steps. *Social Networks*, 5(2):109–137, 1983.
- Pengsheng Ji and Jiashun Jin. Coauthorship and citation networks for statisticians. *The Annals of Applied Statistics*, 10(4):1779–1812, 2016.
- Jiashun Jin. Fast community detection by SCORE. *Annals of Statistics*, 43(1):57–89, 2015.
- Jiashun Jin, Zheng Tracy Ke, and Shengming Luo. Estimating network memberships by simplex vertex hunting. *arXiv preprint arXiv:1708.07852*, 2017.
- Brian Karrer and M. E. J. Newman. Stochastic blockmodels and community structure in networks. *Physical Review E*, 83(1):16107, 2011.

- Jérôme Kunegis. Konect: the koblenz network collection. In *Proceedings of the 22nd international conference on world wide web*, pages 1343–1350, 2013.
- Andrea Lancichinetti and Santo Fortunato. Community detection algorithms: a comparative analysis. *Physical Review E*, 80(5):056117, 2009.
- Jing Lei and Alessandro Rinaldo. Consistency of spectral clustering in stochastic block models. *Annals of Statistics*, 43(1):215–237, 2015.
- Lihua Lei. Unified  $\ell_{2 \rightarrow \infty}$  eigenspace perturbation theory for symmetric random matrices. *arXiv preprint arXiv:1909.04798*, 2019.
- Woosang Lim, Rundong Du, and Haesun Park. Codinmf: Co-clustering of directed graphs via nmf. In *AAAI*, pages 3611–3618, 2018.
- Wangqun Lin, Xiangnan Kong, Philip S Yu, Quanyuan Wu, Yan Jia, and Chuan Li. Community detection in incomplete information networks. In *Proceedings of the 21st International Conference on World Wide Web*, pages 341–350, 2012.
- Xueyu Mao, Purnamrita Sarkar, and Deepayan Chakrabarti. On mixed memberships and symmetric nonnegative matrix factorizations. *International Conference on Machine Learning*, pages 2324–2333, 2017.
- Xueyu Mao, Purnamrita Sarkar, and Deepayan Chakrabarti. Overlapping clustering models, and one (class) svm to bind them all. In *Advances in Neural Information Processing Systems*, volume 31, pages 2126–2136, 2018.
- Xueyu Mao, Purnamrita Sarkar, and Deepayan Chakrabarti. Estimating mixed memberships with sharp eigenvector deviations. *Journal of the American Statistical Association*, pages 1–13, 2020.
- Mohamed Ndaoud, Suzanne Sigalla, and Alexandre B Tsybakov. Improved clustering algorithms for the bipartite stochastic block model. *IEEE Transactions on Information Theory*, 68(3):1960–1975, 2021.
- M. E. J. Newman. Coauthorship networks and patterns of scientific collaboration. *Proceedings of the National Academy of Sciences*, 101(suppl 1):5200–5205, 2004.
- Richard A Notebaart, Frank HJ van Enkevort, Christof Francke, Roland J Siezen, and Bas Teusink. Accelerating the reconstruction of genome-scale metabolic networks. *BMC Bioinformatics*, 7:296, 2006.
- Clara Pizzuti. Ga-net: A genetic algorithm for community detection in social networks. In *International Conference on Parallel Problem Solving from Nature*, pages 1081–1090. Springer, 2008.
- Tai Qin and Karl Rohe. Regularized spectral clustering under the degree-corrected stochastic blockmodel. *Advances in Neural Information Processing Systems 26*, pages 3120–3128, 2013.

- Zahra S. Razaee, Arash A. Amini, and Jingyi Jessica Li. Matched bipartite block model with covariates. *Journal of Machine Learning Research*, 20(34):1–44, 2019.
- Karl Rohe, Tai Qin, and Bin Yu. Co-clustering directed graphs to discover asymmetries and directional communities. *Proceedings of the National Academy of Sciences of the United States of America*, 113(45):12679–12684, 2016.
- John Scott and Peter J. Carrington. *The SAGE handbook of social network analysis*. London: SAGE Publications, 2014.
- Ulrich Stelzl, Uwe Worm, Maciej Lalowski, Christian Haenig, Felix H Brembeck, Heike Goehler, Martin Stroedicke, Martina Zenkner, Anke Schoenherr, Susanne Koeppen, et al. A human protein-protein interaction network: a resource for annotating the proteome. *Cell*, 122(6):957–968, 2005.
- Gang Su, Allan Kuchinsky, John H Morris, David J States, and Fan Meng. Glay: community structure analysis of biological networks. *Bioinformatics*, 26(24):3135–3137, 2010.
- Joel A. Tropp. User-friendly tail bounds for sums of random matrices. *Foundations of Computational Mathematics*, 12(4):389–434, 2012.
- Zhe Wang, Yingbin Liang, and Pengsheng Ji. Spectral algorithms for community detection in directed networks. *Journal of Machine Learning Research*, 21(153):1–45, 2020.
- Yuan Zhang, Elizaveta Levina, and Ji Zhu. Detecting overlapping communities in networks using spectral methods. *SIAM Journal on Mathematics of Data Science*, 2(2):265–283, 2020.
- Zhixin Zhou and Arash A.Amini. Analysis of spectral clustering algorithms for community detection: the general bipartite setting. *Journal of Machine Learning Research*, 20(47):1–47, 2019.
- Zhixin Zhou and Arash A. Amini. Analysis of spectral clustering algorithms for community detection: the general bipartite setting. *arXiv preprint arXiv:1803.04547*, 2018.
- Zhixin Zhou and Arash A Amini. Optimal bipartite network clustering. *J. Mach. Learn. Res.*, 21(40):1–68, 2020.